Alkene-Coordinated Palladium(0) Cross-Coupling Precatalysts: Comparing Oxidative Addition and Catalytic Reactivity for Dimethyl Fumarate and Maleic Anhydride Stabilizing Ligands

Gilian T. Thomas,[†] Jared Z. Litman,[†] Binh Dang Ho,[†] Jingjun Huang,[†] Kalina Blonska,[†] Nathan D. Schley,[‡] and David C. Leitch[†]*

[†]Department of Chemistry, University of Victoria, Victoria, British Columbia V8P 5C2, Canada.
[‡]Department of Chemistry, Vanderbilt University, Nashville, Tennessee 37235, United States.

* To whom correspondence should be addressed: dcleitch@uvic.ca

ABSTRACT: Air-stable palladium (0) precatalysts are advantageous for facilitating a variety of chemical transformations, and are desirable precursors for high-throughput experimentation studies. We report investigations into air-stable Pd(0) precatalysts stabilized by dimethyl fumarate (DMFU) as an electron-deficient alkene. A Pd(0) DMFU complex with a diazabutadiene (DAB) supporting ligand readily undergoes substitution with both monodentate and bidentate phosphines to form phosphine–Pd–DMFU complexes *in situ*. These complexes undergo oxidative addition with ArBr substrates, and are also effective precatalysts for Heck coupling, Suzuki-Miyaura coupling, and Miyaura borylation. Catalytic comparisons of the DAB–Pd–DMFU precursor to other Pd sources reveals benefits and limitations of this system, including high activity in Heck coupling, and challenges with *in situ* catalyst generation.

INTRODUCTION

Metal-catalyzed cross-coupling is one of the most widely used approaches in organic synthesis,[1–3] enabling the formation of new carbon-element bonds. These transformations are critical to the synthesis of many pharmaceuticals,[4–6] materials,[7] and agrochemicals,[8] as well as other fine chemicals. While great strides have been made in developing non-precious metal catalysts for these reactions, organopalladium catalysis remains the most versatile and widely applicable approach, particularly in complex molecule synthesis. An obvious drawback is the low abundance and corresponding high cost of palladium, requiring processes to drive toward minimizing the quantities required. As a result, extensive catalyst and condition screening campaigns are common when developing a Pd-catalyzed reaction to identify the most active possible system. There is thus a need for palladium compounds that are active precursors to catalytic species *and* suitable for microscale high-throughput experimentation (HTE).[9–13]

Generally, HTE screening takes place using a combination of a Pd source and added ancillary ligand (e.g. PR$_3$) to form the desired catalyst *in situ*.[14–18] This maximizes the potential ligand space available for screening. Another approach is to use single-component precatalysts that already contain the desired ancillary ligand.[19–22] These can be more operationally convenient and also more active, though not all desired ancillary ligands are available as part of commercial precatalysts. In both cases, the oxidation state of the Pd precursor is important. Cross-coupling catalysis is generally initiated by a Pd(0) species undergoing oxidative addition with the electrophilic substrate; therefore, *in situ* systems and single-component precatalysts must rapidly and reliably convert to an appropriate Pd(0) species. This is either achieved through reduction of a Pd(II) precursor, or by directly using a Pd(0) precursor. There are many prior examples of Pd(II) sources and precatalysts, whereas Pd(0) precursors are less common.[21–23] Key examples of Pd(0) sources for cross-coupling catalysis include Pd$_2$dba$_3$ (and its crystalline solvates) for *in situ* generation,[14,15,24–27] and homoleptic Pd(PR$_3$)$_n$ complexes, including Pd(PPh$_3$)$_4$, as single-component catalysts (Figure 1A).[28,29]

More recently, we and others have investigated alternative Pd(0) sources (Figure 1B). Early work from Beller and co-workers identified diallyl ether as a chelating diene to stabilize a Pd(0) complex for Suzuki coupling.[30] The Buchwald group has also reported a series of dipalladium complexes with bridging COD ligands that accommodate exceptionally bulky phosphines.[31–33] Frantz and co-workers reported a chiral single-component Pd(0) precatalyst (BobCat) that takes advantage of a water-soluble dba derivative to promote catalysis.[34] Sato, Kanbara, and Kuwabara used an alternative strategy to generate an air-stable Pd(0) species by using a highly electron-deficient phosphine PAr$^F_3$ (Ar^F = 3,5-bis(trifluoromethyl)phenyl).[35,36]

1

In 2021 we reported [DMP]DAB–Pd–MAH (1) as a convenient and active Pd(0) source designed specifically to enable HTE studies ([DMP]DAB = *N*,*N*'-bis(2,6-dimethylphenyl)diazabutadiene; MAH = maleic anhydride).[37] A key strength of this complex is its rapid and quantitative ligand substitution chemistry, enabling reliable *in situ* formation of phosphine–Pd–MAH species for a wide range of phosphine ligands during catalysis.[38,39] We further isolated and characterized several of these phosphine–Pd–MAH complexes, and used them as active single-component precatalysts (Figure 1C).[37,40] Contemporaneously, Fantasia and co-workers reported a series of phosphine–Pd–DVDS complexes (DVDS = 1,3-divinyl-1,1,3,3-tetramethyldisiloxane), and also demonstrated their efficiency as single-component precatalysts.[41]

A *Simple Pd(0) sources for catalysis*

Pd(PPh$_3$)$_4$ Pd(PR$_3$)$_2$ R = *o*-tol, Cy, *t*Bu, *etc.*

Pd$_2$dba$_3$ • solvent   solvent = dba, CHCl$_3$, PhH, *etc.*

B *Single-component Pd(0) precatalysts*

L$_n$Pd [O] **Beller 2000**   L$_n$Pd—[cyclooctadiene]—PdL$_n$ **Buchwald 2013**   (Ar^F)$_3$P–Pd–PCy$_3$ **Kanbara and Kuwabara 2020**

L$_n$Pd [Me$_2$Si-O-SiMe$_2$] **Fantasia 2021**   [Cy$_2$P...Pd...OMe] **Frantz 2018** CO$_2$Na
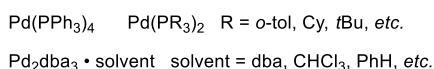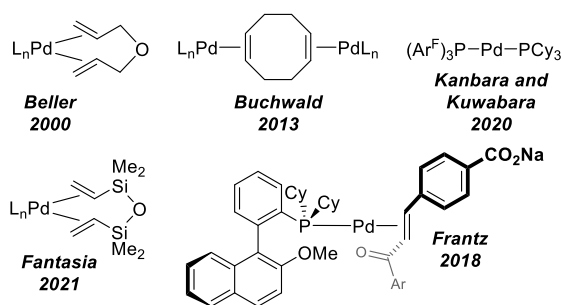
C [DMP]*DAB-Pd-MAH as a versatile Pd(0) precursor*

1
[DMP]**DAB-Pd-MAH**
→ (R$_3$P)$_n$—Pd—[maleic anhydride]
Active precatalysts for cross-coupling and allylation catalysis
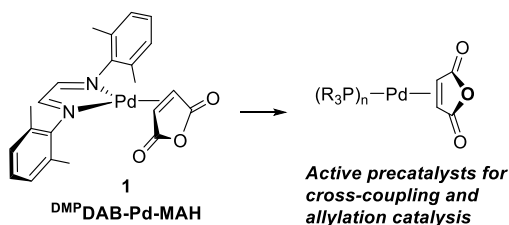
D *This work: Pd(0) DMFU complexes in cross-coupling*

2
[4-An]**DAB-Pd-DMFU**
→ (R$_3$P)$_n$—Pd—[DMFU] CO$_2$Me, MeO$_2$C
Oxidative addition reactivity Comparisons to MAH precats.
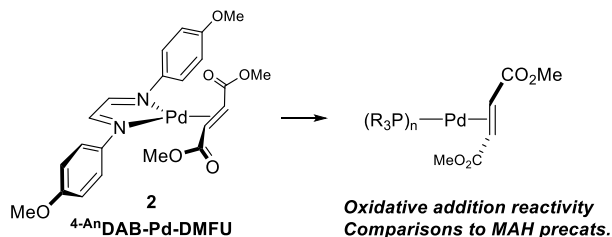
Figure 1. Pd(0) complexes used as precatalysts for cross-coupling reactions. **A**) Simple homoleptic Pd(0) sources used in cross-coupling. **B**) Single-component phosphine–Pd–alkene complexes reported as precatalysts. **C**) Diazabutadiene (DAB) palladium(0) complex [DMP]DAB–Pd–MAH (**1**) and corresponding single-component precatalysts previously reported by us.[37] **D**) Analogous [4-An]DAB–Pd–DMFU (**2**) complex first reported by Vrieze and co-workers,[42] and use to generate phosphine–Pd–DMFU precatalysts.

Herein we report our studies of diazabutadiene (DAB) and phosphine Pd(0) dimethylfumarate (DMFU) complexes in the context of cross-coupling catalysis and high-throughput experimentation. Our hypothesis was that the less stabilizing DMFU ligand would lead to increased catalytic activity compared to MAH-based precatalysts. We have therefore studied the previously reported [4-An]DAB–Pd–DMFU (**2**) complex as a Pd(0) precursor, and prepared a series of single-component phosphine–Pd–DMFU precatalysts (Figure 1D).

RESULTS AND DISCUSSION

Synthesis and Characterization of Pd–DMFU Complexes with DAB and Phosphine Ligands. α-Diimine ligands are well-studied in organopalladium chemistry, most notably for Pd(II) olefin polymerization catalysts.[43–58] Corresponding Pd(0) complexes with the DAB-variant of α-diimines (derived from glyoxyl) have also been previously studied,[42,59] including as precatalysts in Heck coupling,[60–64] catalytic alkyne hydrogenation,[65–69] methoxycarbonylation of styrene,[70,71] and the synthesis of carbohydrate derivatives.[72] Furthermore, several (R$_3$P)$_2$Pd–DMFU complexes are known, either with simple monophosphines,[73–77] or with chelating phosphines.[78–89] This work provides important structural and synthetic guidance toward candidate Pd(0) precatalysts. Specifically, many different synthetic routes are used to access these compounds, including reduction of L$_n$Pd(allyl)X species in the presence of DMFU, coordination of DMFU to Pd(PR$_3$)$_n$ complexes, or ligand substitution using Pd$_2$dba$_3$.

In 1981, Vrieze and co-workers reported two DAB–Pd–DMFU complexes that we identified as potential Pd(0) sources for cross-coupling catalysis: [tBu]DAB–Pd–DMFU and [4-An]DAB–Pd–DMFU (**2**).[42] We prepared the former compound using both of the procedures described, including using "Pd$_3$(TTAA)$_3$" (which is actually Pd$_2$dta$_3$, dta = ditoluylideneacetone, as identified by Echavarren and Stille[90]); however, we quickly eliminated this compound as a candidate precursor due to its laborious synthesis and purification. As described by Vrieze and co-workers, it is "very soluble in many organic solvents and … extremely labile".[42] In contrast, **2** is readily prepared in high yield largely due to its very low solubility in the reaction solvent. Unfortunately, this also complicates its characterization; Vrieze and co-workers did not report NMR spectroscopic data for **2**. In our case, we were able to collect a suitable ^{1}H NMR spectrum of **2**, confirming the proposed structure; however, its solubility in CDCl$_3$ was determined to be only 2.13 mg/mL, preventing acquisition of ^{13}C NMR spectra.

To assess if **2** could be a precursor for *in situ* catalyst formation, we examined its ligand substitution chemistry with several phosphines (Table 1). Stirring a suspension of **2** in CH$_2$Cl$_2$ with 2 equiv of a monophosphine or 1 equiv of a bis(phosphine) displaces [4-An]DAB to generate the corresponding phosphine–Pd–DMFU complex. Solution yields of these species were determined by ^{1}H NMR spectroscopy. After 2 h, DPPF, BippyPhos, and P(*o*-tol)$_3$ formed complexes in >90% yields (Table 1, entries 1–3), whereas XPhos, XantPhos and DPEPhos furnished their respective Pd complexes in modest yields ranging from 65–79% (Table 1, entries 4–6). Notably, these latter three examples exhibit considerably slower ligand substitution than what we previously observed with [DMP]DAB–Pd–MAH (complete in minutes). This is likely due to the poorer solubility of **2** leading to slower reaction rates.

2

Table 1. Phosphine metalation of $^{4\text{-An}}$DAB–Pd–DMFU assessed by ^{1}H NMR spectroscopy.[a]
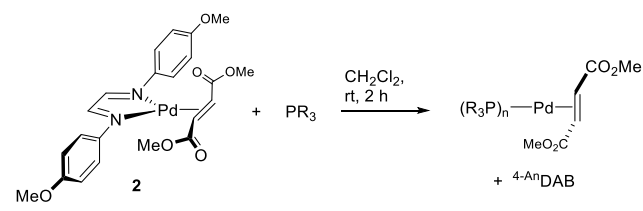
Entry	Phosphine	Yield (%)[a]
1	P(o-tol)$_3$	99
2	BippyPhos	91
3	DPPF	91
4	XPhos	79
5	DPEPhos	67
6	XantPhos	65

[a]Conditions: **2** (0.1 mmol), phosphine (0.2 mmol), CH$_2$Cl$_2$ (3 mL), rt, 2 h under inert atmosphere. [a]Crude yields were assessed by ^{1}H NMR using 1,3,5-trimethoxybenzene as an internal standard.

Attempts to isolate these phosphine complexes from the reaction between **2** and phosphines was very challenging. While we were able to achieve high solution yields with longer reaction times, purification was complicated by the near identical solubilities of the desired Pd complex and the $^{4\text{-An}}$DAB byproduct. Attempts at selective extraction and precipitation/crystallization led to low yields and/or impure material. We instead investigated chromatographic purification. In one case, we were able to reliably prepare the **XPhos–Pd–DMFU** complex from the reaction of **2** and XPhos (eq. 1). Purification by flash chromatography achieved separation of the $^{4\text{-An}}$DAB byproduct, giving the desired complex in 82% yield. Unfortunately, all other investigated complexes co-eluted with $^{4\text{-An}}$DAB due to its propensity to "streak" on the silica gel. We could partly alleviate this by complexing the $^{4\text{-An}}$DAB byproduct with ZnBr$_2$ after ligand substitution, followed by flash chromatography; however this method gave variable and generally lower yields due to challenges with chromatography.

(1)
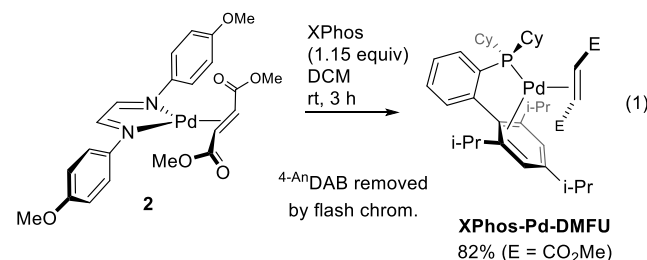
While these purification issues are not important in the context of *in situ* catalyst formation, we required an alternative and more general means to access single-component phosphine–Pd–DMFU complexes for structural and reactivity comparisons. We therefore prepared five complexes *via* ligand substitution from Pd$_2$dba$_3$•CHCl$_3$ (Scheme 1).

Fortunately, removal of the dba byproduct is feasible through precipitation of the complex, followed by extraction of the soluble dba from the crude solid. In addition to the complex derived from heterobiaryl phosphine BippyPhos, we also isolated four complexes with chelating bis(phosphine) ligands: DPEPhos, XantPhos, *rac*-BINAP, and DPPF. Isolated yields of

Scheme 1. Synthesis and isolation of (phosphine)–Pd-DMFU complexes from Pd$_2$dba$_3$•CHCl$_3$.[a]
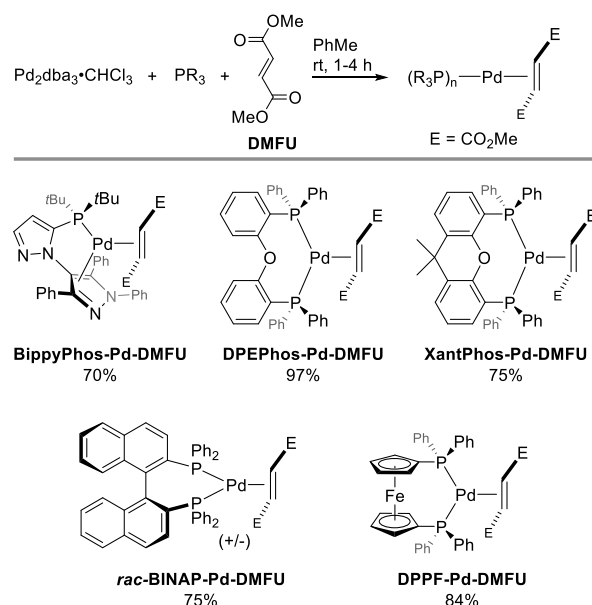
[a]Conditions: Pd$_2$dba$_3$ (0.04 mmol), phosphine (0.09 mmol), dimethyl fumarate (0.11 mmol), PhMe (9 mL), rt, 1-4 h under inert atmosphere. Yields are reported after isolation by trituration with hexane or pentane.

these complexes are good to excellent (70-97%). All six complexes are air stable, and were isolated under ambient atmosphere. The solubility of these phosphine complexes is also much improved compared to **2**, enabling full characterization by NMR spectroscopy and high-resolution mass spectrometry. Three complexes were also characterized by X-ray crystallography, with the solid state molecular structures of ***rac*-BINAP–Pd–DMFU**, **DPEPhos–Pd–DMFU**, and **DPPF–Pd–DMFU** shown in Figure 2.

Table 2 displays a comparison of selected bond lengths and angles for two pairs of bis(phosphine)–Pd–alkene complexes, with data for the MAH complexes from our prior work.[37] Despite the change in electron-accepting character of the alkene, from a stronger π-acid (MAH) to a weaker one (DMFU), the metrical parameters are nearly identical when comparing complexes with the same phosphine ligand. The Pd–P lengths are statistically identical, and the P–Pd–P bite angles are also very similar for the DPPF pair. Notably, the DPEPhos–Pd–DMFU complex does have a tighter bite angle than the MAH analogue by 3°; this is due to a slight conformation change in the ligand between these two complexes in the solid state. The Pd–C bond lengths are only slightly longer in the DMFU complexes compared to their MAH counterparts; however, this is barely statistically significant.

In both sets of complexes, the alkene C=C bond is significantly elongated from the free alkene length (solid state C=C lengths: MAH = 1.303 Å;[91] DMFU = 1.318 Å[92]). The Δ(C=C length) is approx. 0.9-1 Å, consistent with considerable back donation from a filled *d*-symmetry orbital on Pd. There is no clear distinction between the two alkenes in terms of elongation; in fact, the less electron-deficient DMFU experiences *greater* elongation than MAH when coordinated to Pd(0).

3

BINAP-Pd-DMFU[a]

DPEPhos-Pd-DMFU[b]
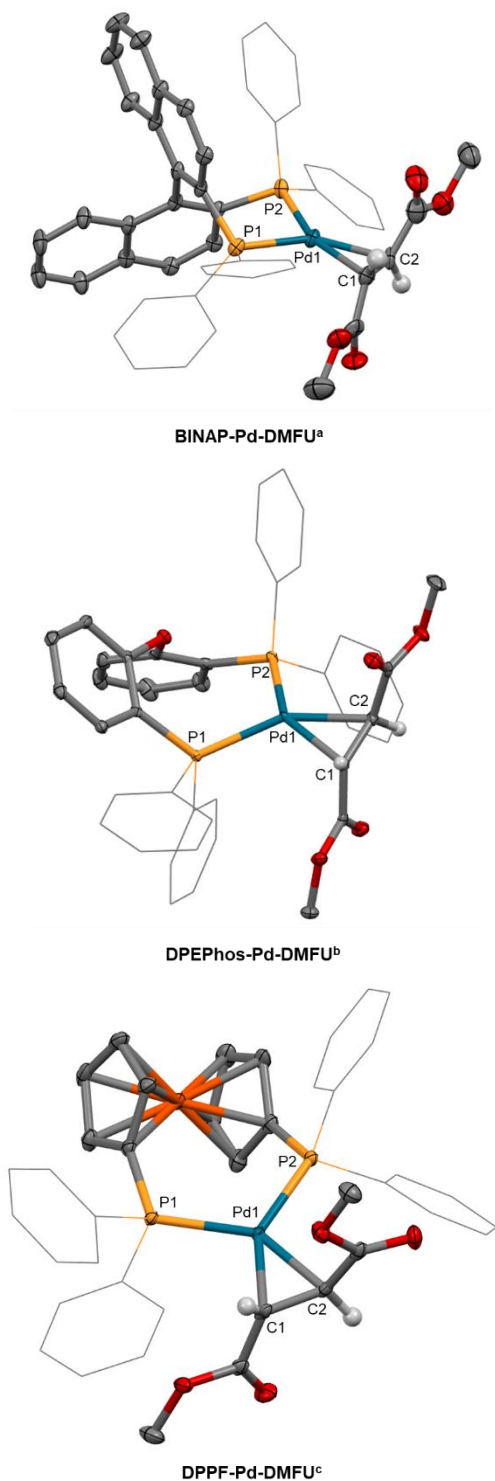
DPPF-Pd-DMFU[c]

Figure 2. Solid state molecular structures of **BINAP–Pd–DMFU**, **DPEPhos–Pd–DMFU**, and **DPPF–Pd–DMFU**. Ellipsoids plotted at 50% probability; phenyl rings on phosphine ligands shown as wireframe for clarity; H atoms except those on alkene removed for clarity. Note that C1 and C2 are defined as the two alkene carbons in the DMFU ligand; atom numbering may be different in Supporting Information tables and CIFs. [a]Molecule disordered over two positions; one orientation shown. [b]Disordered CHCl$_3$ solvent molecule not shown. [c]One of two independent molecules in the asymmetric unit is shown; disordered pentane molecule not shown.

Table 2. Selected bond lengths (Å) and angles (°) from solid-state molecular structures of DPEPhos–Pd–MAH,[37] DPEPhos–Pd–DMFU, DPPF–Pd–MAH,[37] and DPPF–Pd–DMFU.

	DPEPhos–Pd–MAH[a]	DPEPhos–Pd–DMFU[b]	DPPF–Pd–MAH[a]	DPPF–Pd–DMFU[b]
Pd1–P1	2.3140(10)	2.3140(5)	2.324(4)	2.3204(7)
Pd1–P2	2.3211(10)	2.3157(5)	2.302(4)	2.3243(7)
Pd1–C1	2.104(4)	2.146(2)	2.140(16)	2.127(3)
Pd1–C2	2.125(4)	2.124(2)	2.105(16)	2.144(3)
C1–C2	1.396(6)	1.428(3)	1.39(2)	1.422(4)
P1–Pd1–P2	106.32(3)	103.559(19)	105.16(13)	106.23(3)
C1–Pd1–C2	38.55(15)	39.08(8)	38.3(6)	38.89(11)
C1–Pd1–P1	106.38(12)	108.31(6)	113.5(5)	105.67(8)
C2–Pd1–P2	108.67(12)	108.45(6)	102.9(5)	109.20(8)

[a]C1 and C2 are defined as the two alkene carbons in the MAH ligand.[37] [b]C1 and C2 are defined as the two alkene carbons in the DMFU ligand; note that atom numbering may be different in Supporting Information tables and CIFs.

Oxidative addition reactivity of Pd(0) DMFU complexes. Our major impetus for investigating Pd(0) DMFU complexes is that the higher lability of the DMFU ligand should result in increased catalytic reactivity. In particular, we wanted to be able to access Pd(II) oxidative addition complexes directly from phosphine-ligated Pd(0) alkene complexes. Isolable oxidative addition complexes are "on-cycle" precatalysts, and are also useful in late-stage modification of pharmaceuticals and biomolecules.[93–96] Often, these complexes are made from homoleptic Pd(PR$_3$)$_n$ precursors (for simple phosphines),[97–100] or from *in situ* combinations of phosphine ligands and Pd$_2$dba$_3$ or (COD)PdR$_2$ species.[94,101,14,102,103]

A seemingly ideal scenario to access Pd(II) oxidative addition complexes is to use Pd(0) precursors with the desired phosphine ligand already installed, such as phosphine–Pd–alkene. Disappointingly, all attempts to observe oxidative addition between our previously reported phosphine–Pd–MAH complexes and a variety of aryl bromide substrates at elevated temperatures have been unsuccessful. We attribute this to ground-state stabilization of the Pd(0) complex by the strongly π-acidic MAH ligand leading to unfavorable thermodynamics for MAH dissociation, and thus very low concentration of (R$_3$P)$_n$Pd(0).

To test our hypothesis that higher DMFU lability would lead to improved oxidative addition reactivity, we treated several phosphine–Pd–DMFU complexes with excess 4-bromoacetophenone at elevated temperature (Scheme 2). In contrast to the aforementioned MAH complexes, we do observe oxidative addition reactivity. For XPhos, the desired Pd(II) complex is formed in 41% solution yield after 8 h; however, unreacted **XPhos–Pd–DMFU** is still present, and prolonged reaction times result in decomposition. For BippyPhos and DPPF, the oxidative addition complexes are isolable in 81% and 70% yield respectively. We also re-tested the corresponding Pd(0) MAH complexes under otherwise identical conditions, with no reaction observed. Thus, single-component phosphine–Pd–DMFU complexes provide a convenient pathway to oxidative addition complexes for mechanistic and/or synthetic studies.

Scheme 2. Synthesis of oxidative addition complexes from $(R_3P)_n$–Pd–DMFU.[a]
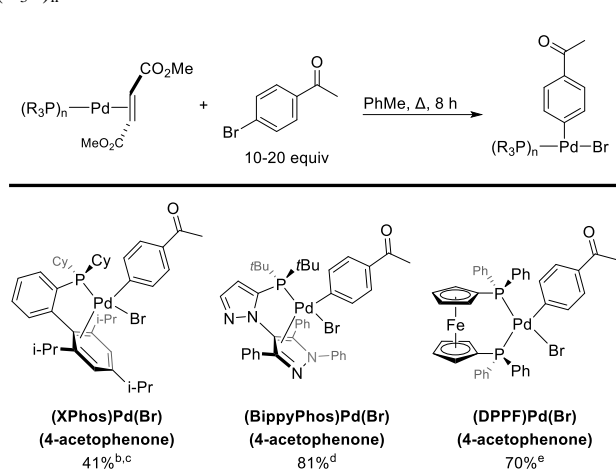
[a]Conditions: $(R_3P)_n$–Pd–DMFU (0.025 mmol), ArBr (0.25 mmol), PhMe (1 mL). [b]Conditions: XPhos–Pd–DMFU (0.014 mmol), ArBr (0.28 mmol), PhMe (1 mL). [c]Solution yield assessed by ^{1}H NMR spectroscopy using 1,3,5-trimethoxybenzene as internal standard, rxn temp. 85 °C. [d]Isolated yield, rxn temp. 60 °C. [e]Isolated yield, rxn temp. 80 °C.

Catalytic evaluation for Heck coupling. To evaluate the catalytic reactivity of **2** and the phosphine–Pd–DMFU complexes derived therefrom, we conducted a series of comparisons using three exemplar coupling reactions: Heck coupling, Suzuki-Miyaura coupling, and Miyaura borylation. In each case, we performed microscale screening of **2** alongside 3 other Pd precursors – Pd$_2$dba$_3$•CHCl$_3$, Pd(OAc)$_2$, and **1** – for *in situ* catalyst formation. Follow-up validation experiments on larger scale provides further comparison under more synthetically relevant conditions.

First, we assessed a Heck coupling reaction between 4-bromoacetophenone and methyl methacrylate under conditions analogous to those initially reported by Littke and Fu.[104] We previously used this reaction as a comparator when evaluating the ^{DMP}DAB–Pd–MAH precursor **1**, which is roughly equal in activity to Pd$_2$dba$_3$•CHCl$_3$ when paired with P(t-Bu)$_3$.[37] A 24-reaction screen involving six ligands, including P(t-Bu)$_3$ alongside other simple mono and bidentate phosphines, reveals that complex **2** is an effective Pd precursor for this reaction (Figure 3). Using only 2 mol% Pd, the top hits are **2**/P(t-Bu)$_3$ and Pd$_2$dba$_3$•CHCl$_3$/P(t-Bu)$_3$. Interestingly, two other ligands – P(o-tol)$_3$ and JohnPhos – give reasonable conversion to the product when paired with **2** or Pd$_2$dba$_3$•CHCl$_3$. Pd(OAc)$_2$ and especially complex **1** perform relatively poorly, missing these ligand hits. These data contrast with those from our prior work on **1**, where the microscale array was performed with much higher catalyst loading (13 mol%).

To validate these screening results, we performed this Heck reaction on 3-fold larger scale, and 4-fold increased concentration (Table 3). Here, we observe the formation of the bis-arylated alkene as an overreaction product. With the higher concentration, **1** is now a viable precursor, exhibiting slightly increased solution yield of the Heck product relative to **2** when paired with P(t-Bu)$_3$; however, we also observe slightly more overreaction product with **1** (4.3:1 for **1** versus 5.7:1 for **2**, entries 1-2).
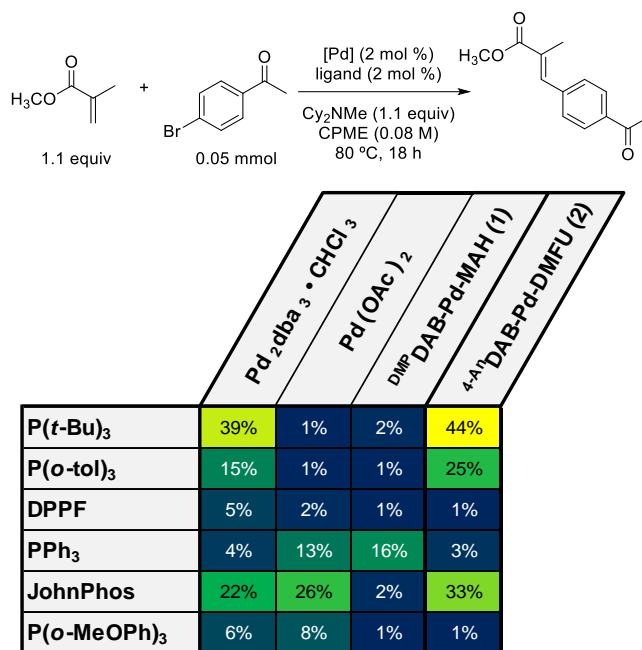
Figure 3. Microscale screening results for the Heck reaction between 4-bromoacetophenone and methyl methacrylate using 4 Pd sources and 6 ligands.

	Pd$_2$dba$_3$•CHCl$_3$	Pd(OAc)$_2$	^{DMP}DAB-Pd-MAH (1)	$^{4-Anis}$DAB-Pd-DMFU (2)
P(t-Bu)$_3$	39%	1%	2%	44%
P(o-tol)$_3$	15%	1%	1%	25%
DPPF	5%	2%	1%	1%
PPh$_3$	4%	13%	16%	3%
JohnPhos	22%	26%	2%	33%
P(o-MeOPh)$_3$	6%	8%	1%	1%

Table 3. Hit validation and comparison of **1** and **2** as Pd sources for the Heck reaction between 4-bromoacetophenone and methyl methacrylate on larger scale and at higher concentration.

Entry	Pd Source	Ligand	*mono-Ar* Yield (%)[a]	*bis-Ar* Yield (%)[a]
1	**1**	P(t-Bu)$_3$	52	12
2	**2**	P(t-Bu)$_3$	40	7
3	**1**	P(o-tol)$_3$	7	0
4	**2**	P(o-tol)$_3$	90	10
5	**1**	JohnPhos	6	0
6	**2**	JohnPhos	27	7
7	Pd(P(o-tol)$_3$)$_2$	none	64	21

[a]Solution yield determined by ^{1}H NMR spectroscopy using 1,3,5-trimethoxybenzene as an internal standard.

Strikingly, DMFU-based **2** performs much better than **1** with P(o-tol)$_3$ as the ligand, achieving 90% yield versus only 7% respectively (entries 3-4). The product ratio is also 9:1, outperforming all other conditions as well as our prior results with **1** (6:1 mono/bis).[37] JohnPhos also performs better when paired with **2**, albeit both results are poor relative to P(o-tol)$_3$ (entries

5

5-6). Finally, we hypothesized that the combination of **2** and P(*o*-tol)$_3$ may simply be generating the known (and commercially available) Pd(P(*o*-tol)$_3$)$_2$ homoleptic Pd(0) complex *in situ*; however, use of this complex as a precatalyst gives poorer yield and selectivity relative to the **2**/ P(*o*-tol)$_3$ combination. As well, ^{31}P NMR spectroscopy of a 1:1 molar ratio of **2** and P(*o*-tol)$_3$ indicates Pd(P(*o*-tol)$_3$)$_2$ is not present. Here, we hypothesize that the 1:1 Pd/P ratio, as well as the presence of DMFU as a stabilizing ligand, modulates the reactivity for maximum mono-arylation selectivity.

To further compare the reactivity of **1** and **2** as precursors, we monitored product formation over time during the early stages of the reaction (Figure 4). In particular, we wanted to identify any potential induction periods due to slow phosphine metalation and/or alkene dissociation. For **1**, we observe essentially no product during the 4 h reaction time, consistent with the low yield observed after 18 h (Table 3, entry 3). With **2**, we observe no induction period, with maximum rate occurring at the beginning of the reaction, confirming that the **2**/P(*o*-tol)$_3$ combination rapidly generates a catalytically active Pd species. In contrast, **1** appears to be essentially inactive under these conditions, presumably due to the presence of the stronger binding and therefore inhibitory MAH ligand. Finally, small quantities of the bis-arylated product only become observable at 4 h using **2**, with a mono:bis product ratio of 9:1, consistent with the final selectivity ratio (Table 3, entry 4).
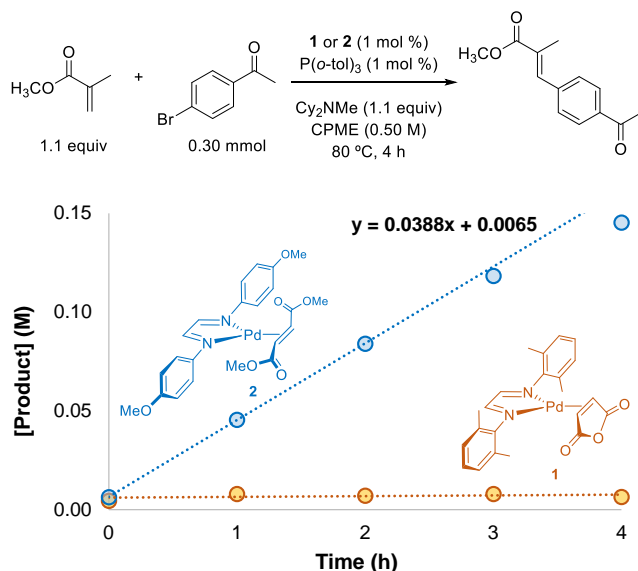
Figure 4. Reaction progress monitoring for initial rate of Heck coupling of 4-bromoacetophenone and methyl methacrylate comparing **1** and **2** as Pd precursors combined with P(*o*-tol)$_3$. No significant induction period is observed for **2**/P(*o*-tol)$_3$. Conditions: Ar–Br (0.30 mmol), methyl methacrylate (0.33 mmol), [Pd] (0.0030 mmol), P(*o*-tol)$_3$ (0.003 mmol), *N,N*-dicyclohexylmethyl-amine (0.33 mmol), CPME (0.60 mL), 80 ºC, 4 h, under inert atmosphere. Yield determined by ^{1}H NMR spectroscopy using 1,3,5-trimethoxybenzene as an internal standard.

Catalytic evaluation for Suzuki-Miyaura coupling. Next, we evaluated the Suzuki-Miyaura coupling between 2-chloro-5-methylpyridine and phenylboronic acid, which we previously tested with **1**/XPhos.[37] We observed that **1** was inferior to Pd(OAc)$_2$ as a precursor for this reaction, and hypothesized that

use of a less strongly bound alkene (*i.e.* DMFU) should lead to improved reactivity, as observed for the Heck reaction described above.

Under microscale screening conditions with low Pd loading (2 mol%), low concentration (0.08 M in limiting reagent) and short reaction time (2 h), we observe that both **1** and **2** are equal or inferior to the standard Pd sources Pd$_2$dba$_3$•CHCl$_3$ and Pd(OAc)$_2$. This is especially striking with XPhos, where **1** and **2** produce about 5-fold lower yield than Pd$_2$dba$_3$•CHCl$_3$. SPhos, P(*t*-Bu)$_3$, and RuPhos give comparable product yields regardless of the Pd source, while PPh$_3$ appears to work best with Pd(OAc)$_2$ (perhaps due to formation of alternative catalyst species[105]). Overall, there is little difference between the two DAB-based precursors (**1** and **2**), despite the different alkene stabilizing ligands.

	Pd$_2$dba$_3$•CHCl$_3$	Pd(OAc)$_2$	^{DMF}DAB-Pd-MAH (1)	4-Ar^{n}DAB-Pd-DMFU (2)
XPhos	64%	27%	14%	11%
SPhos	35%	25%	28%	46%
PPh$_3$	13%	58%	41%	16%
DPPF	27%	20%	7%	2%
P(*t*-Bu)$_3$	26%	26%	34%	31%
RuPhos	45%	56%	34%	39%
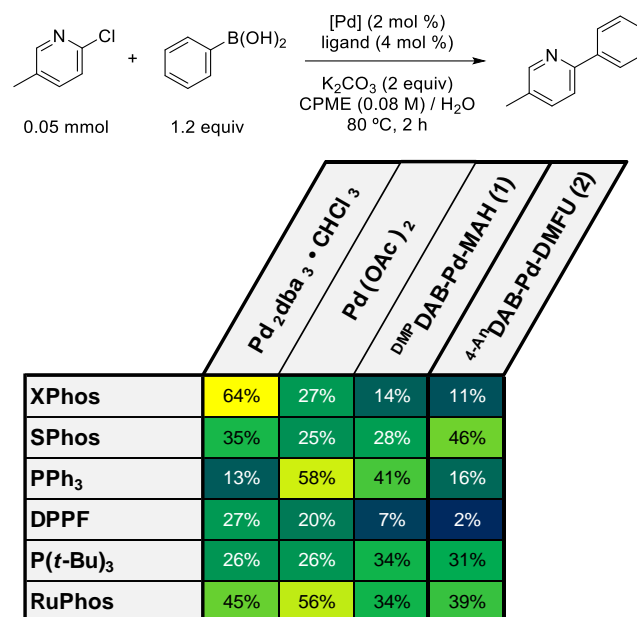
Figure 5. Microscale screening results for the Suzuki-Miyaura reaction between 2-chloro-5-methylpyridine and phenylboronic acid using 4 Pd sources and 6 ligands.

Evaluating **1** and **2** on larger scale and higher concentration reinforces their similar reactivity (Table 4). As a baseline, Pd$_2$dba$_3$•CHCl$_3$ / XPhos gives 70% solution yield of the product after 18 hours, whereas **1** performs better (98%) and **2** performs similarly (71%) (entries 1-3). Complex **1** is again superior to **2** when paired with SPhos (entries 4-5) or RuPhos (entries 8-9), while both precursors enable only modest conversion with P(*t*-Bu)$_3$ (entries 6-7). Clearly, using DMFU as a more weakly coordinating alkene does not lead to increased catalytic activity in this case, contrary to our catalyst design hypothesis and in stark contrast to the Heck coupling results.

To directly compare the catalytic reaction rates between **1** and **2** as Pd precursors for this reaction, and to identify any potential induction periods, we monitored the concentration of product over the first 4 hours. These reactions were also performed at lower temperature (50 °C) in an effort to accentuate any reactivity differences. Using the *in situ* combination of **1** or **2** and XPhos (2 equiv XPhos per Pd) leads to dramatically different outcomes. While **1**/XPhos does not exhibit any clear induction

6

period, reaching ~10% product after 4 hours, **2**/XPhos leads to poor conversion over this time period. Only at 4 hours is >1% product observed.

Table 4. Hit validation and comparison of **1** and **2** as Pd sources for the Heck reaction between Suzuki-Miyaura reaction between 2-chloro-5-methylpyridine and phenylboronic acid on larger scale and at higher concentration.
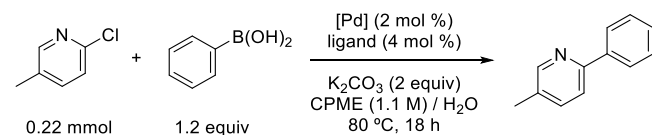
Entry	[Pd]	Ligand	Yield (%)[a]
1	Pd$_2$dba$_3$·CHCl$_3$	XPhos	70
2	**1**	XPhos	98
3	**2**	XPhos	71
4	**1**	SPhos	73
5	**2**	SPhos	62
6	**1**	P(t-Bu)$_3$	20
7	**2**	P(t-Bu)$_3$	36
8	**1**	RuPhos	79
9	**2**	RuPhos	67

[a]Solution yield determined by ^{1}H NMR spectroscopy using ferrocene as an internal standard.
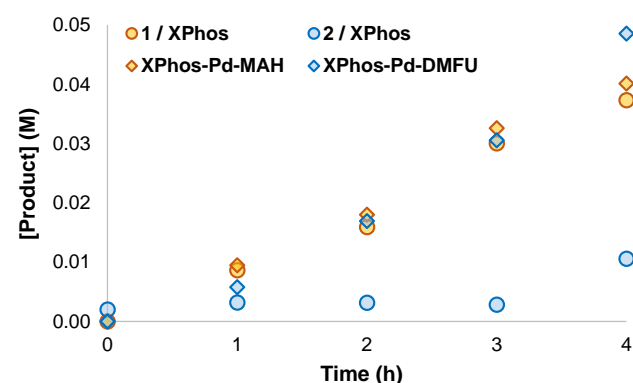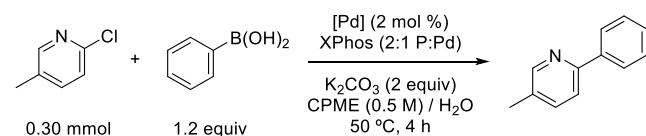
Figure 6. Reaction progress monitoring for initial rate of Suzuki-Miyaura coupling of 2-chloro-5-methylpyridine and phenylboronic acid comparing **1** and **2** as Pd precursors combined with XPhos, as well as the corresponding **XPhos–Pd–MAH** and **XPhos–Pd–DMFU** single-component precatalysts. Conditions: 2-chloro-5-methylpyridine (0.30 mmol), phenylboronic acid (0.36 mmol), [Pd] (0.006 mmol), XPhos (0.012 mmol for *in situ* catalyst formation, 0.006 mmol for single-component precatalysts), K$_2$CO$_3$ (0.60 mmol), CPME (0.60 mL), degassed H$_2$O (0.40 mL).

To determine the source of this induction period for **2**, we compared these reaction profiles to those obtained with single-component precatalysts **XPhos–Pd–MAH**[37] and **XPhos–Pd–DMFU** (both with added XPhos to keep the P:Pd ratio consistent at 2:1). For the MAH precatalyst, an identical initial rate is observed to the *in situ* system, which is consistent with our prior observation of rapid phosphine metalation through ligand substitution of **1**. For the DMFU precatalyst, the single-component system significantly outperforms the *in situ* system, with a near-identical rate to the two MAH-containing catalysts. Thus, we propose the induction period observed for **2**/XPhos is not due to slow dissociation of DMFU prior to oxidative addition, but rather slow ligand substitution to generate XPhos–Pd–DMFU due to the low solubility of **2**.

Catalytic evaluation for Miyaura borylation. Pd-catalyzed borylation of aryl (pseudo)halides is another reaction that often requires extensive catalyst screening to achieve selective synthesis.[6,106–109] We previously evaluated **1** alongside other common Pd sources for the catalytic borylation of alkenyl carboxylate substrates, with **1** underperforming relative to Pd(OAc)$_2$.[110] Here, we tested a more typical borylation of an unactivated aryl bromide using B$_2$pin$_2$, with 2-ethylhexanoic acid as a rate-enhancing additive (Figure 7).[107,109] Microscale screening of this reaction reveals that Pd(OAc)$_2$ does outperform the three Pd(0) sources with dppb and Xantphos, possibly due to formation of alternative, more reactive catalyst species through phosphine-mediated reduction pathways.[111] However, simple monodentate phosphines (PPh$_3$, P(o-MeOPh)$_3$) perform better with Pd$_2$dba$_3$•CHCl$_3$ or **1**. On larger scale and higher concentration, **1** and **2** perform well with both of these ligands, outperforming the Pd$_2$dba$_3$•CHCl$_3$ / PPh$_3$ system (Table 5). In this reaction, as for the Suzuki-Miyaura coupling, the switch from an MAH-stabilized to DMFU-stabilized precatalyst does not make a significant difference in overall reactivity.
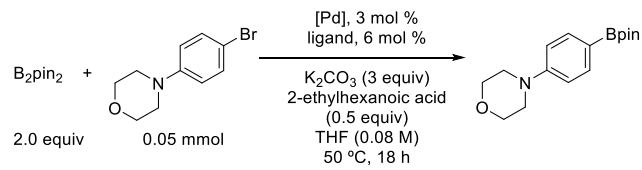
	Pd$_2$dba$_3$•CHCl$_3$	Pd(OAc)$_2$	^{DMP}DAB-Pd-MAH (1)	$^{4-An}$DAB-Pd-DMFU (2)
dppb	17%	51%	37%	8%
XantPhos	20%	68%	15%	43%
dppf	11%	49%	23%	5%
PPh$_3$	68%	54%	72%	68%
DPEPhos	47%	73%	67%	65%
P(o-MeOPh)$_3$	81%	66%	79%	65%

Figure 7. Microscale screening results for the Miyaura borylation of *N*-(4-bromophenyl)-morpholine using 4 Pd sources and 6 ligands.

7

Table 5. Hit validation and comparison of **1** and **2** as Pd sources for the Miyaura borylation of *N*-(4-bromophenyl)-morpholine on larger scale and at higher concentration.
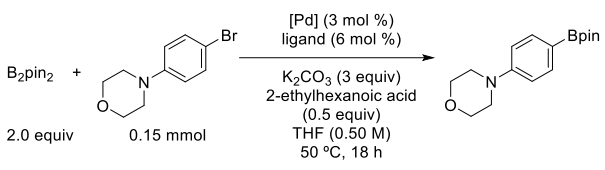
Entry	[Pd]	Ligand	Yield (%)[a]
1	Pd₂dba₃·CHCl₃	PPh₃	67
2	**1**	PPh₃	98
3	**2**	PPh₃	99
4	Pd₂dba₃·CHCl₃	P(*o*-MeOPh)₃	83
5	**1**	P(*o*-MeOPh)₃	77
6	**2**	P(*o*-MeOPh)₃	85

[a]Solution yield determined by ^{1}H NMR spectroscopy using 1,3,5-trimethoxybenzene as an internal standard.

Catalytic evaluation for C–O coupling and insights into catalyst activation. One of the reactions for which **1** was identified as a very effective precursor is alcohol arylation.[37] Prior screening revealed BippyPhos as a suitable ligand, with **1**/BippyPhos and the corresponding **BippyPhos–Pd–MAH** precatalyst outperforming other state-of-the-art precursors. To assess the effect of incorporating DMFU as an alternative stabilizing ligand on this reaction, we monitored the arylation of *n*-butanol with 4-bromoacetophenone at low Pd loading (Figure 8). Consistent with the previously observed reactivity, **1**/BippyPhos and **BippyPhos–Pd–MAH** are excellent precatalysts, reaching >95% solution yield after only 3 hours. In stark contrast, **2**/BippyPhos and **BippyPhos–Pd–DMFU** are worse, forming only 5% and 15% product respectively.

This result is completely counterintuitive based solely on a consideration of alkene binding strength. Furthermore, this result *and* the previously observed parity of activity between **1** and **2** (and/or precatalysts derived therefrom) for the Suzuki-Miyaura and Miyaura borylation reactions are inconsistent with the oxidative addition reactivity described previously: Lₙ–Pd–MAH complexes are inert toward thermal oxidative addition with Ar–Br substrates, whereas the corresponding Lₙ–Pd–DMFU complexes convert to the on-cycle LₙPd(Ar)(Br) species. Two questions arise from these conflicting observations: how can MAH-based precatalysts operate at all if oxidative addition is so sluggish, and how can they perform equally well or even significantly better than DMFU analogues?

The contrasting results between the Heck coupling (Figure 4) and the C–O coupling (Figure 8) provide a possible explanation (Scheme 3). In the Heck reaction, the reactivity trends are consistent with alkene binding strength as the major factor: MAH is a likely strong competitive inhibitor, stabilizing off-cycle Pd(0) species to a greater extent than the weaker-binding DMFU. The major difference in the C–O coupling conditions is the presence of a stronger nucleophile and base. MAH is a reactive acid anhydride, readily undergoing ring-opening esterification by alcohol nucleophiles; here, *n*- butanol.[112] This would convert the strongly-binding MAH into a monobutyl maleate anion, which is more electron-rich and therefore a weaker alkene ligand for Pd(0). Similarly, MAH is readily hydrolyzed to

maleic acid salts in reactions with inorganic or aqueous bases, such as Suzuki-Miyaura coupling and Miyaura borylation.
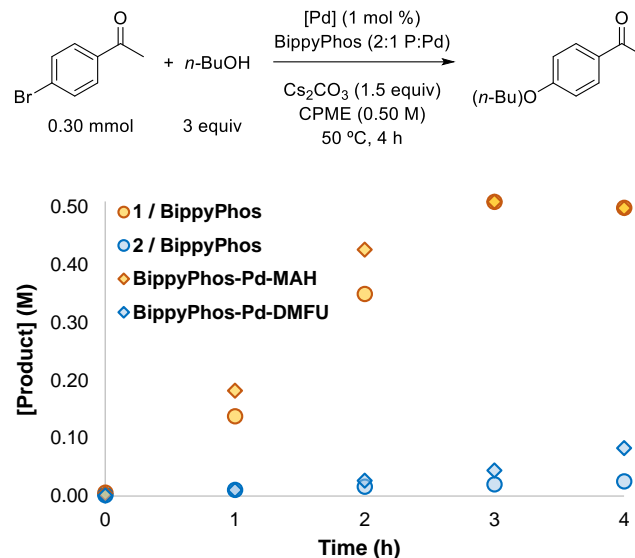
Figure 8. Reaction progress monitoring for C–O coupling between 4-bromoacetophenone and *n*-butanol comparing **1** and **2** as Pd precursors combined with BippyPhos, as well as the corresponding **BippyPhos–Pd–MAH** and **BippyPhos–Pd–DMFU** single-component precatalysts. Conditions: 4-bromoacetophenone (0.30 mmol), *n*-butanol (0.90 mmol), [Pd] (0.003 mmol), BippyPhos (0.006 mmol for *in situ* catalyst formation, 0.003 mmol for single-component precatalysts), Cs₂CO₃ (0.45 mmol), CPME (0.60 mL), 50 ºC, 4 h under inert atmosphere.

Scheme 3. Proposed precatalyst activation pathways for DMFU-stabilized and MAH-stabilized complexes toward oxidative addition.
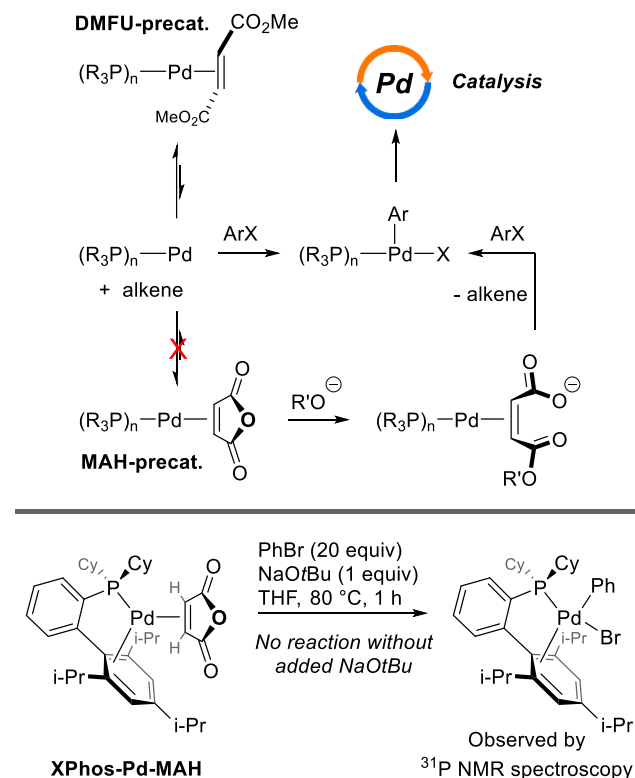
To test if the presence of a base and/or nucleophile could activate L$_n$–Pd–MAH complexes toward oxidative addition, and thus increase their catalytic activity, we examined the reaction of **XPhos–Pd–MAH** with PhBr under a variety of conditions. In THF at 80 °C (sealed vial), **XPhos–Pd–MAH** (0.010 mmol) is unreactive toward 20 equiv of PhBr, with only starting materials observed after 1 h. Under analogous conditions, addition of NaO*t*Bu (0.010 mmol, 1 equiv per Pd) does result in the formation of the known[113] oxidative addition complex (42% ^{31}P NMR spectroscopy peak area), with unreacted **XPhos–Pd–MAH** (22%) and free XPhos (36%) also observed (along with Pd black formation). While more in-depth investigations are ongoing to fully elucidate the activation mechanisms for MAH-stabilized precatalysts, it is clear that simple alkene dissociation is not the primary pathway in catalytic reactions involving stronger bases and/or nucleophiles.

CONCLUSIONS

Overall, DAB–Pd–alkene complexes **1** and **2** are effective Pd(0) precursors for *in situ* catalyst generation during cross-coupling reactions. DMFU-stabilized complex **2** undergoes ligand substitution with a variety of catalytically-relevant phosphines to generate the corresponding phosphine–Pd–DMFU complexes; however, isolation of these single-component precatalysts is better achieved from Pd$_2$dba$_3$•CHCl$_3$ due to challenges removing the diazabutadiene byproduct. In contrast to our previously reported phosphine–Pd–MAH complexes, these DMFU complexes undergo thermal oxidative addition with an Ar–Br substrate. This reactivity difference is due to weaker Pd–DMFU coordination compared to Pd–MAH. This effect manifests as improved catalytic reactivity for the DMFU-stabilized systems in a model Heck reaction, where **2** significantly outperforms **1** when paired with P(*o*-tol)$_3$.

However, in other catalytic reactions including Suzuki-Miyaura coupling and Miyaura borylation, the DMFU and MAH systems are indistinguishable in terms of catalytic activity. In C–O coupling, **1** significantly outperforms **2** when paired with BippyPhos; the superiority of the MAH-based system is also evident when comparing the single-component BippyPhos–Pd–alkene precatalysts. These results point to alternative activation pathways available to the MAH-based systems, which we propose involve ring-opening acyl substitution of MAH with the base and/or nucleophile present in these latter coupling reactions. In-depth mechanistic elucidation of these and other catalyst activation pathways are currently underway.

EXPERIMENTAL SECTION

General Considerations. All solvents and common organic reagents were purchased from commercial suppliers and used without further purification. All palladium sources (except Pd$_2$dba$_3$•CHCl$_3$ and ^{DMP}DAB–Pd–MAH) were purchased from Strem Chemicals and used as received. Pd$_2$dba$_3$•CHCl$_3$ was prepared according to the method of Zalesskiy and Ananikov,[25] and $^{4-An}$DAB–Pd–DMFU was synthesized using the method of Vrieze and co-workers.[42] ^{DMP}DAB–Pd–MAH (**1**) and (R$_3$P)$_n$–Pd–MAH complexes were prepared by our previously reported protocols.[37] N,N'-bis(2,6-dimethylphenyl)ethan-1,2-diimine and N,N'-bis(4-methoxy)ethan-1,2-diimine were prepared using reported procedures.[114,115] All phosphine ligands were purchased from Strem Chemicals and used as received. Anhydrous solvents (SureSeal) were purchased from MilliporeSigma and used as received. All air-free manipulations were performed under a dry N$_2$ atmosphere using an MBraun glovebox. Heating/stirring for vial-scale experiements was

achieved using rare-earth magnetic tumble stirrers acquired from V&P Scientific. All NMR spectra were acquired on either a Bruker AVANCE 300 MHz spectrometer or a Bruker AVANCE Neo 500 MHz spectrometer. All ^{1}H and ^{13}C NMR chemical shifts are referenced to residual protio-solvents, and ^{31}P NMR chemical shifts are referenced to H$_3$PO$_4$ (85%) as an external standard. All NMR spectroscopic data is processed using Mestrenova. High-resolution electrospray ionization mass spectrometry (HRESI-MS) was performed on a Bruker Maxis Impact or ThermoScientific Ultimate 3000 ESI-Orbitrap Exactive Plus.

BINAP–Pd–DMFU. Under nitrogen atmosphere, a 9-dram vial was charged with Pd$_2$dba$_3$•CHCl$_3$ (0.05 mmol, 50.0 mg), toluene (8 mL), and a stir bar. A solution of *rac*-BINAP (0.11 mmol, 66 mg) in 3 mL toluene was added dropwise, and the solution stirred for 5 minutes. Then, dimethyl fumarate (0.14 mmol, 20.1 mg) in toluene (1 mL) was added in one portion. The reaction mixture was vigorously stirred for 4 hours, during which the solution color changed from maroon to pale yellow. The following steps were performed under ambient atmosphere. The solvent was removed under reduced pressure, yielding a viscous yellow oil. The oil was then dissolved in minimal dichloromethane, passed through a pipette filter to remove any palladium black impurities, and the solvent evaporated under reduced pressure. Hexanes (2 mL) was added to precipitate the crude product, which was then evaporated to dryness. The crude product was then collected over a fine frit and washed with hexanes (~200 mL) until washings were colorless and excess phosphine had been removed. The product was then dried *in vacuo* for 12 hours, yielding **BINAP–Pd–DMFU** as a fine pale-yellow powder (60 mg, 75%). ^{1}H NMR (500 MHz, CDCl$_3$) δ 7.93 – 7.85 (m, 4H), 7.50 – 7.42 (m, 10H), 7.36 (d, *J* = 8.7 Hz, 2H), 7.29 – 7.24 (m, 4H), 7.12 (ddt, *J* = 11.3, 6.6, 1.4 Hz, 4H), 7.04 (ddd, *J* = 8.3, 6.8, 1.4 Hz, 2H), 6.77 (dd, *J* = 8.6, 1.0 Hz, 2H), 6.68 – 6.63 (m, 2H), 6.50 (t, *J* = 7.5 Hz, 4H), 4.10 (d, *J* = 6.2 Hz, 2H), 3.14 (s, 6H). ^{31}P (202 MHz, CDCl$_3$) δ 28.2 (major diastereomer), 28.7 (minor diastereomer). ^{13}C NMR (125 MHz, CDCl$_3$) δ 173.29, 134.96, 134.90, 134.15, 133.74, 133.45, 133.02, 129.91, 128.81, 128.56, 128.29, 128.25, 128.21, 127.85, 127.75, 127.54, 127.32, 126.91, 126.87, 126.17, 125.82, 55.71, 55.55, 50.50. HRESI-MS: *m/z* for C$_{50}$H$_{41}$O$_4$P$_2$Pd [M+H]$^+$: calculated 873.1509; found 873.1503.

BippyPhos–Pd–DMFU. Under nitrogen atmosphere, a 9-dram vial was charged with Pd$_2$dba$_3$•CHCl$_3$ (0.039 mmol, 40.0 mg), anhydrous toluene (8 mL), and a stir bar. A solution of BippyPhos (0.085 mmol, 42.9 mg) in 2 mL toluene was added dropwise, and the solution stirred for 5 minutes. Then, dimethyl fumarate (0.11 mmol, 16.1 mg) in toluene (1 mL) was added in one portion. The reaction mixture was vigorously stirred for 4 hours, during which the solution color changed from maroon to pale yellow. All of the following steps were performed under ambient air. The solvent was removed under reduced pressure, yielding a viscous orange oil. The oil was dissolved in minimal dichloromethane, passed through a pipette filter to remove any palladium black impurities, and the solvent evaporated under reduced pressure. Hexanes (2 mL) was added to precipitate the crude product, which was then evaporated to dryness under reduced pressure. The crude product was then triturated with pentanes (10 x 4 mL) until washings were colorless and the resulting powder was chromatographically pure, as indicated by thin layer chromatography (2:1 Hex/EtOAc). The product was then dried *in vacuo* for 12 hours, yielding BippyPhos–Pd–DMFU as a fine yellow-orange powder (41.2 mg, 70%). ^{1}H NMR (500 MHz, CD$_2$Cl$_2$) δ 8.03 (d, J = 2.0 Hz, 1H, -CH=N), 7.76 – 7.72 (m, 2H, Ar-H), 7.50 – 7.46 (m, 2H, Ar-H), 7.40 – 7.34 (m, 3H, Ar-H), 7.30 – 7.19 (m, 8H, Ar-H), 6.61 (d, J = 2.1 Hz, 1H, -CH=C), 3.98 (br, 2H, CH=CH), 3.53 (s, 6H, O-CH$_3$), 1.00 (d, J = 14.8 Hz, 9H, -(CH$_3$)$_3$), 0.65 (d, J = 14.7 Hz, 9H, -(CH$_3$)$_3$). ^{31}P NMR (202 MHz, CD$_2$Cl$_2$) δ 43.5. ^{13}C NMR (125 MHz, CD$_2$Cl$_2$) δ 171.72, 150.92, 145.36, 144.41, 144.36, 140.18, 139.17, 131.89, 131.39, 129.99, 129.22, 129.09, 128.76, 128.68, 128.44, 128.21, 128.04, 126.16, 113.28, 108.58, 50.99, 34.88, 34.78, 34.47, 34.38, 29.80, 29.73, 29.04, 28.97. HRESI-MS: *m/z* for C$_{38}$H$_{44}$N$_4$O$_4$PPd [M+H]$^+$: calculated 757.2144; found 757.2147.

DPEPhos–Pd–DMFU. Under nitrogen atmosphere, a 9-dram vial was charged with Pd$_2$dba$_3$•CHCl$_3$ (0.039 mmol, 40.0 mg), toluene (8 mL), and a stir bar. A solution of DPEPhos (0.085 mmol, 45.8 mg) in 2 mL toluene was added dropwise, and the solution stirred for 5 minutes. Then, dimethyl fumarate (0.11 mmol, 16.1 mg) in toluene (1

9

mL) was added all at once. The reaction mixture was vigorously stirred for 1 hour, during which the solution color changed from maroon to pale yellow. The following steps were performed under ambient air. The solvent was removed under reduced pressure, yielding a viscous yellow oil. The oil was then dissolved in minimal dichloromethane, passed through a pipette filter to remove palladium black impurities, and the solvent evaporated under reduced pressure. Hexanes (2 mL) was added to precipitate the crude product, which was then evaporated to dryness. The crude product was then triturated with hexanes (8 x 4 mL) until washings were colorless. The product was then dried *in vacuo* for 12 hours, yielding DPEPhos–Pd–DMFU as a fine pale-yellow powder (59.4 mg, 97%). ^{1}H NMR (500 MHz, CD$_2$Cl$_2$) δ 7.43 – 7.34 (m, 10H, Ar-*H*), 7.29 – 7.21 (m, 10H, Ar-*H*), 7.14 (td, *J* = 7.7, 1.7 Hz, 2H, Ar-*H*), 6.85 – 6.77 (m, 4H, Ar-*H*), 6.48 (td, *J* = 8.0, 1.7 Hz, 2H, Ar-*H*), 3.86 (d, *J* = 5.0 Hz, 2H, -C*H*=C*H*-), 3.15 (s, 6H, O-C*H₃*). ^{31}P NMR (202 MHz, CDCl$_3$) δ 13.66. ^{13}C NMR (125 MHz, CD$_2$Cl$_2$) δ 172.57, 158.44, 158.36, 135.10, 134.81, 134.11, 134.04, 133.97, 133.91, 133.76, 133.70, 133.64, 133.13, 132.86, 130.86, 129.52, 129.34, 128.21, 128.17, 128.13, 128.08, 126.73, 126.50, 124.13, 120.30, 57.51, 57.46, 57.30, 57.25, 50.36. HRESI-MS: *m/z* for C$_{42}$H$_{37}$O$_5$P$_2$Pd [M+H]$^+$: calculated 789.1161; found 789.1162.

DPPF–Pd–DMFU. Under nitrogen atmosphere, a 9-dram vial was charged with Pd$_2$dba$_3$•CHCl$_3$ (0.039 mmol, 40.0 mg), toluene (8 mL), and a stir bar. A solution of DPPF (0.085 mmol, 46.9 mg) in 2 mL toluene was added dropwise and the solution was stirred for 5 minutes. Then, dimethyl fumarate (0.11 mmol, 16.1 mg) in toluene (1 mL) was added in one portion. The reaction mixture was vigorously stirred for 2 hours, during which the solution changed from maroon to orange. The following steps were performed under ambient air. The solvent was removed under reduced pressure, yielding a viscous brown oil. The oil was then dissolved in minimal dichloromethane, passed through a pipette filter to remove any palladium black impurities, and evaporated under reduced pressure. Hexanes (2 mL) was added to precipitate the crude product, which was then evaporated to dryness. The crude product was then triturated with hexanes (10 x 4 mL) until washings were colorless. The product was then dried *in vacuo* for 12 hours, yielding DPPF–Pd–DMFU as a fine brown-orange colored powder (52.3 mg, 84%). ^{1}H NMR (500 MHz, CD$_2$Cl$_2$): δ 7.69 (br, 4H, Ar-*H*), 7.57 (br, 4H, Ar-*H*), 7.46 – 7.35 (m, 12H, Ar-*H*), 4.36 (s, 2H, Cp-*H*), 4.29 (d, *J* = 16.8 Hz, 4H, Cp-*H*), 4.05 (d, *J* = 5.0 Hz, 2H, -C*H*=C*H*-), 3.90 (s, 2H, Cp-*H*), 3.14 (s, 6H, O-C*H₃*). ^{31}P NMR (202 MHz, CD$_2$Cl$_2$) δ 20.24. ^{13}C NMR (125 MHz, CD$_2$Cl$_2$): δ 172.67, 139.07, 135.69, 135.62, 135.55, 135.33, 135.06, 133.29, 133.23, 133.17, 130.72, 129.58, 129.36, 128.75, 128.71, 128.67, 128.59, 128.55, 128.52, 75.38, 75.31, 75.23, 73.95, 73.70, 71.08, 55.90, 55.82, 55.75, 55.66, 50.59. HRESI-MS: *m/z* for C$_{40}$H$_{37}$FeO$_4$P$_2$Pd [M+H]$^+$: calculated 805.0563; found 805.0567.

XantPhos–Pd–DMFU. Under nitrogen atmosphere, a 9-dram vial was charged with Pd$_2$dba$_3$•CHCl$_3$ (0.05 mmol, 50.0 mg), toluene (8 mL), and a stir bar. A solution of XantPhos (0.11 mmol, 62 mg) in 3 mL toluene was added dropwise and the solution stirred for 5 minutes. Then, dimethyl fumarate (0.14 mmol, 20.1 mg) in toluene (1 mL) was added in one portion. The reaction mixture was vigorously stirred for 2 hours, during which the solution color changed from maroon to pale yellow. The following steps were performed under ambient air. The solvent was removed under reduced pressure, yielding a viscous yellow oil. The oil was then dissolved in minimal dichloromethane, passed through a pipette filter to remove palladium black impurities, and evaporated under reduced pressure. Hexanes (2 mL) was added to precipitate the crude product, which was then evaporated to dryness. The crude product was then triturated with hexanes (12 x 4 mL) until washings were colorless. The product was then dried *in vacuo* for 12 hours, yielding XantPhos–Pd–DMFU as a fine pale-yellow powder (59 mg, 75 %). ^{1}H NMR (500 MHz, CD$_2$Cl$_2$) δ 7.49 (dd, *J* = 7.7, 1.5 Hz, 2H), 7.35 – 7.24 (m, 13H), 7.19 (td, *J* = 7.7, 1.9 Hz, 5H), 7.11 – 7.00 (m, 6H), 6.37 (td, *J* = 7.5, 1.4 Hz, 2H), 3.85 – 3.79 (m, 2H, -C*H*=C*H*-), 3.24 (s, 6H, O-C*H₃*), 1.60 (s, 6H (R-C*H₃*). ^{31}P NMR (202 MHz, CD$_2$Cl$_2$) δ 9.11. ^{13}C NMR (125 MHz, CD$_2$Cl$_2$) δ 172.56, 156.17, 156.09, 134.95, 134.93, 134.90, 134.69, 134.47, 134.45, 133.94, 133.82, 133.77, 133.65, 131.97, 129.54, 129.44, 128.45, 128.43, 128.38, 128.36, 126.67, 124.35, 124.31, 123.04, 122.84, 58.37, 58.34, 58.17, 58.13,

50.97, 36.38, 27.84. HRESI-MS: *m/z* for C$_{45}$H$_{41}$O$_5$P$_2$Pd [M+H]$^+$: calculated 829.1475; found 829.1480.

XPhos–Pd–DMFU. Under nitrogen atmosphere, a 4-dram vial was charged with $^{4\text{-}An}$DAB–Pd–DMFU (**2**, 0.141 mmol, 75.0 mg), XPhos (0.162 mmol, 77.1 mg) and a stir bar. Degassed dichloromethane (4 mL) was added to dissolve the solids, and the resulting dark brown solution was vigorously stirred for 3 hours. The following steps were performed under ambient air. The solvent was removed under reduced pressure, yielding a brown solid. The crude solid was dissolved in minimum of hexanes/EtOAc and purified *via* column chromatography, 1:0–2:1 hexanes/EtOAc. The resulting yellow solution was concentrated under reduced pressure, yielding a viscous yellow oil. Hexanes (5 mL) was added to the yellow oil and the solvent was removed under reduced pressure, yielding a bright yellow solid of XPhos–Pd–DMFU (84.1 mg, 82%). ^{1}H NMR (500 MHz, CD$_2$Cl$_2$) δ 7.62 (t, *J* = 7.1 Hz, 1H), 7.42 – 7.32 (m, 2H), 7.27 (d, *J* = 1.9 Hz, 1H), 7.09 (d, *J* = 2.0 Hz, 1H), 6.97 – 6.92 (m, 1H), 4.31 (s, 1H), 3.47 (s, 6H), 3.09 (hept, *J* = 7.0 Hz, 1H), 2.43 (s, 1H), 2.25 (hept, *J* = 6.8 Hz, 1H), 2.13 – 1.98 (m, 3H), 1.99 – 1.61 (m, 10H), 1.54 – 1.44 (m, 1H), 1.42 (d, *J* = 6.9 Hz, 3H), 1.35 – 1.18 (m, 16H), 1.16 – 1.01 (m, 2H), 0.92 (d, *J* = 6.7 Hz, 3H), 0.76 (d, *J* = 6.7 Hz, 3H). ^{31}P NMR (202 MHz, CD$_2$Cl$_2$) δ 35.19. ^{13}C NMR (125 MHz, CD$_2$Cl$_2$) δ 147.86, 147.61, 147.36, 143.17, 137.40, 137.22, 137.20, 132.27, 132.19, 129.25, 129.23, 127.05, 127.02, 124.93, 124.89, 122.87, 121.86, 53.85, 53.63, 53.42, 53.20, 52.99, 50.28, 35.84, 35.81, 35.70, 33.66, 31.45, 31.37, 30.31, 30.26, 29.48, 29.43, 29.30, 29.25, 28.86, 27.40, 27.36, 27.30, 27.28, 27.17, 27.11, 27.02, 26.26, 26.14, 25.36, 25.30, 25.20, 23.63, 23.01, 22.07. HRESI-MS: *m/z* for C$_{39}$H$_{58}$O$_4$PPd [M+H]$^+$: 727.3117; found 727.3124.

(DPPF)Pd(Br)(4-Acetophenone). Under nitrogen atmosphere, a 2-dram vial was charged with DPPF–Pd–DMFU (20 mg, 0.025 mmol), 4-bromoacetophenone (49.5 mg, 0.25 mmol) and anhydrous toluene (1 mL). The orange solution was heated at 85 °C for 12 hours, during which a light yellow precipitate gradually formed. Under ambient air, the solvent was removed under reduced pressure, and CPME (1 mL) was added. The mixture was allowed to stand at -20°C for 1 hour. Then, the product was triturated with ice-cold CPME (3 x 3 mL) and hexanes (2 x 2 mL). The resulting solid was placed under vacuum overnight to remove residual solvent, yielding (DPPF)Pd(Br)(4-Acetophenone) as a light yellow powder (14.9 mg, 70%). ^{1}H NMR (500 MHz, CDCl$_3$) δ 8.12 – 7.98 (m, 2H), 7.54 – 7.44 (m, 3H), 7.42 – 7.26 (m, 5H), 7.18 – 7.05 (m, 4H), 4.70 (q, J = 2.1 Hz, 1H), 4.51 (s, 1H), 4.16 (t, J = 1.9 Hz, 1H), 3.64 (q, J = 1.8 Hz, 1H). ^{31}P NMR (202 MHz, CDCl$_3$) δ 29.96 (d, J = 32.9 Hz), 9.48 (d, J = 32.9 Hz). ^{13}C data unavailable due to poor solubility, however 2D NMR data is available in the Supplementary Information. HRESI-MS: *m/z* for C$_{42}$H$_{35}$FeOP$_2$Pd [M − Br]$^+$: calculated 779.0559; found 779.0572.

(BippyPhos)Pd(Br)(4-Acetophenone). Under nitrogen atmosphere, a 2-dram vial was charged with BippyPhos–Pd–DMFU (20 mg, 0.026 mmol), 4-bromoacetophenone (52.5 mg, 0.26 mmol) and anhydrous toluene (1 mL). The yellow solution was heated at 60 ºC for 8 hours, during which time a light yellow precipitate gradually formed. Under ambient air, the solvent was removed under reduced pressure, and CPME (2 mL) was then added. The vial was allowed to stand at -20 ºC for 1 hour before trituration with ice-cold CPME (4 x 2 mL) until washings were colorless. The solid was then triturated with hexanes (2 x 2 mL). The resulting solid was placed under vacuum overnight to remove residual solvent, yielding (BippyPhos)Pd(Br)(4-Acetophenone) as a light yellow powder (17.5 mg, 81%). ^{1}H NMR (500 MHz, CDCl$_3$) δ 8.11 (d, *J* = 2.1 Hz, 1H), 7.80 – 7.71 (m, 2H), 7.60 – 7.50 (m, 4H), 7.45 – 7.27 (m, 9H), 7.24 – 7.12 (m, 4H), 6.69 (d, *J* = 2.1 Hz, 1H), 2.47 (s, 3H), 0.87 (d, *J* = 15.4 Hz, 10H), 0.74 (d, *J* = 15.3 Hz, 9H). ^{31}P NMR (202 MHz, CDCl$_3$) δ 32.07. NMR spectra match literature values.[116]

(XPhos)Pd(Br)(4-Acetophenone). Under nitrogen atmosphere, a 2-dram vial was charged with XPhos–Pd–DMFU (10 mg, 0.014 mmol), 4-bromoacetophenone (54.7 mg, 0.28 mmol), trimethoxybenzene (1.2 mg, 0.007 mmol), and anhydrous toluene (1 mL). The deep yellow solution was heated at 85 ºC for 8 h. Under ambient air, the now deep orange solution was then dried under reduced pressure, and re-dissolved in CDCl$_3$. The NMR solution yield of (XPhos)Pd(Br)(4-Acetophenone) was 41%, and NMR data match literature values.[116]

10

Catalytic reaction progress monitoring. A 1.5 mL crimp cap HPLC vial was charged with 0.3 mmol of solid substrates, [Pd], and solid base. Under nitrogen atmosphere, ligand was weighed and added to the vial. Anhydrous CPME was then added, and the vial was capped and removed from of the glovebox. If substrate(s) and/or base was liquid at room temperature they were added after the solvent. The vials were placed in an aluminum block heated to the appropriate temperature inside a tumble stirrer. At each time point, a 27.5 G needle was used to withdraw approximately 50 uL of the reaction mixture through the septum. This aliquot was transferred to a 1-dram vial, and dried using a centrifugal evaporator. NMR spectra acquired in CDCl₃.

Supporting Information

Full tables of screening data, NMR and HRMS spectra, and XRD details. (PDF)

CIFs for **BINAP–Pd–DMFU**, **DPEPhos–Pd–DMFU**, and **DPPF–Pd–DMFU** are deposited with the CCDC with deposition numbers CCDC 2329876-2329878.

Notes

The authors declare the following competing interest: ^{DMP}DAB–Pd–MAH is commercially available from MilliporeSigma (product number 922889), from which the authors may receive royalty payments.

REFERENCES

(1)   Johansson Seechurn, C.; Carin, C.; Kitching, M. O.; Colacot, T. J.; Snieckus, V. Palladium-Catalyzed Cross-Coupling: A Historical Contextual Perspective to the 2010 Nobel Prize. *Angew. Chem. Int. Chem.* **2012**, *51*, 5062–5085. https://doi.org/10.1002/anie.201107017.

(2)   Campeau, L. C.; Hazari, N. Cross-Coupling and Related Reactions: Connecting Past Success to the Development of New Reactions for the Future. *Organometallics* **2019**, *38*. https://doi.org/10.1021/acs.organomet.8b00720.

(3)   Buchwald, S. L.; Hartwig, J. F. In Praise of Basic Research as a Vehicle to Practical Applications: Palladium-Catalyzed Coupling to Form Carbon-Nitrogen Bonds. *Isr. J. Chem.* **2020**, *60*, 177–179. https://doi.org/10.1002/ijch.201900167.

(4)   Brown, D. G.; Boström, J. Analysis of Past and Present Synthetic Methodologies on Medicinal Chemistry: Where Have All the New Reactions Gone? *J. Med. Chem.* **2016**, *59*, 4443–4458. https://doi.org/10.1021/acs.jmedchem.5B01409.

(5)   Ruiz-Castillo, P.; Buchwald, S. L. Applications of Palladium-Catalyzed C–N Cross-Coupling Reactions. *Chem. Rev.* **2016**, *116*, 12564–12649. https://doi.org/10.1021/acs.chemrev.6b00512.

(6)   Magano, J.; Dunetz, J. R. Large-Scale Applications of Transition Metal-Catalyzed Couplings for the Synthesis of Pharmaceuticals. *Chem. Rev.* **2011**, *111*, 2177–2250. https://doi.org/10.1021/cr100346g.

(7)   Baker, M. A.; Tsai, C.-H.; Noonan, K. J. T. Diversifying Cross-Coupling Strategies, Catalysts and Monomers for the Controlled Synthesis of Conjugated Polymers. *Chem. Eur. J.* **2018**, *24*, 13078–13088. https://doi.org/10.1002/chem.201706102.

(8)   Devendar, P.; Qu, R.-Y.; Kang, W.-M.; He, B.; Yang, G.-F. Palladium-Catalyzed Cross-Coupling Reactions: A Powerful Tool for the Synthesis of Agrochemicals. *J. Agric. Food Chem.* **2018**, *66*, 8914–8934. https://doi.org/10.1021/acs.jafc.8b03792.

(9)   Buitrago Santanilla, A.; Regalado, E. L.; Pereira, T.; Shevlin, M.; Bateman, K.; Campeau, L.-C.; Schneeweis, J.; Berritt, S.; Shi, Z.-C.; Nantermet, P.; Liu, Y.; Helmy, R.; Welch, C. J.; Vachal, P.; Davies, I. W.; Cernak, T.; Dreher, S. D. Nanomole-Scale High-Throughput Chemistry for the Synthesis of Complex Molecules. *Science* **2015**, *347*, 49–53. https://doi.org/10.1126/science.1259203.

(10)   Allen, C. L.; Leitch, D. C.; Anson, M. S.; Zajac, M. A. The Power and Accessibility of High-Throughput Methods for Catalysis Research. *Nat. Catal.* **2019**, *2*, 2–4. https://doi.org/10.1038/s41929-018-0220-4.

(11)   Mennen, S. M.; Alhambra, C.; Allen, C. L.; Barberis, M.; Berritt, S.; Brandt, T. A.; Campbell, A. D.; Castañón, J.; Cherney, A. H.; Christensen, M.; Damon, D. B.; Eugenio de Diego, J.; García-Cerrada, S.; García-Losada, P.; Haro, R.; Janey, J.; Leitch, D. C.; Li, L.; Liu, F.; Lobben, P. C.; MacMillan, D. W. C.; Magano, J.; McInturff, E.; Monfette, S.; Post, R. J.; Schultz, D.; Sitter, B. J.; Stevens, J. M.; Strambeanu, I. I.; Twilton, J.; Wang, K.; Zajac, M. A. The Evolution of High-Throughput Experimentation in Pharmaceutical Development and Perspectives on the Future. *Org. Process Res. Dev.* **2019**, *23*, 1213–1242. https://doi.org/10.1021/acs.oprd.9b00140.

(12)   Shevlin, M. Practical High-Throughput Experimentation for Chemists. *ACS Med. Chem. Lett.* **2017**, *8*, 601–607. https://doi.org/10.1021/acsmedchemlett.7b00165.

(13)   Krska, S. W.; DiRocco, D. A.; Dreher, S. D.; Shevlin, M. The Evolution of Chemical High-Throughput Experimentation To Address Challenging Problems in Pharmaceutical Synthesis. *Acc. Chem. Res.* **2017**, *50*, 2976–2985. https://doi.org/10.1021/acs.accounts.7b00428.

(14)   Amatore, C.; Broeker, G.; Jutand, A.; Khalil, F. Identification of the Effective Palladium(0) Catalytic Species Generated in Situ from Mixtures of Pd(dba)₂ and Bidentate Phosphine Ligands. Determination of Their Rates and Mechanism in Oxidative Addition. *J. Am. Chem. Soc.* **1997**, *119*, 5176–5185. https://doi.org/10.1021/ja9637098.

(15)   Amatore, C.; Jutand, A. Role of dba in the Reactivity of Palladium(0) Complexes Generated in Situ from Mixtures of Pd(dba)₂ and Phosphines. *Coord. Chem. Rev.* **1998**, *178–180*, 511–528. https://doi.org/10.1016/S0010-8545(98)00073-3.

(16)   Norton, D. M.; Mitchell, E. A.; Botros, N. R.; Jessop, P. G.; Baird, M. C. A Superior Precursor for Palladium(0)-Based Cross-Coupling and Other Catalytic Reactions. *J. Org. Chem.* **2009**, *74*, 6674–6680. https://doi.org/10.1021/jo901121e.

(17)   Melvin, P. R.; Nova, A.; Balcells, D.; Dai, W.; Hazari, N.; Hruszkewycz, D. P.; Shah, H. P.; Tudge, M. T. Design of a Versatile and Improved Precatalyst Scaffold for Palladium-Catalyzed Cross-Coupling: (η³-1-tBu-Indenyl)₂(μ-Cl)₂Pd₂. *ACS Catal.* **2015**, *5*, 3680–3688. https://doi.org/10.1021/acscatal.5b00878.

(18)   Leitch, D. C.; Becica, J. 13.12 - High-Throughput Experimentation in Organometallic Chemistry and Catalysis. In *Comprehensive Organometallic Chemistry IV*; Parkin, G., Meyer, K., O'Hare, D., Eds.; Elsevier: Oxford, 2022; pp 502–555. https://doi.org/10.1016/B978-0-12-820206-7.00111-6.

(19)   Bruno, N. C.; Tudge, M. T.; Buchwald, S. L. Design and Preparation of New Palladium Precatalysts for C–C and C–N Cross-Coupling Reactions. *Chem. Sci.* **2013**, *4*, 916–920. https://doi.org/10.1039/C2SC20903A.

(20)   Renom-Carrasco, M.; Lefort, L. Ligand Libraries for High Throughput Screening of Homogeneous Catalysts. *Chem. Soc. Rev.* **2018**, *47*, 5038–5060. https://doi.org/10.1039/C7CS00844A.

(21)   Hazari, N.; Melvin, P. R.; Beromi, M. M. Well-Defined Nickel and Palladium Precatalysts for Cross-Coupling. *Nat. Rev. Chem.* **2017**, *1*, 0025. https://doi.org/10.1038/s41570-017-0025.

(22)   Shaughnessy, K. H. Development of Palladium Precatalysts That Efficiently Generate LPd(0) Active Species. *Isr. J. Chem.* **2020**, *60*, 180–194. https://doi.org/10.1002/ijch.201900067.

(23)   Firsan, S. J.; Sivakumar, V.; Colacot, T. J. Emerging Trends in Cross-Coupling: Twelve-Electron-Based L₁Pd(0) Catalysts, Their Mechanism of Action, and Selected Applications. *Chem. Rev.* **2022**, *122*, 16983–17027. https://doi.org/10.1021/acs.chemrev.2c00204.

(24)   Takahashi, Y.; Ito, T.; Sakai, S.; Ishii, Y. A Novel Palladium(0) Complex; Bis(Dibenzylideneacetone)Palladium(0). *J. Chem. Soc. Chem. Commun.* **1970**, 1065–1066. https://doi.org/10.1039/C29700001065.

(25) Zalesskiy, S. S.; Ananikov, V. P. Pd$_2$(dba)$_3$ as a Precursor of Soluble Metal Complexes and Nanoparticles: Determination of Palladium Active Species for Catalysis and Synthesis. *Organometallics* **2012**, *31*, 2302–2309. https://doi.org/10.1021/om201217r.

(26) Janusson, E.; Zijlstra, H. S.; Nguyen, P. P. T.; MacGillivray, L.; Martelino, J.; McIndoe, J. S. Real-Time Analysis of Pd$_2$(dba)$_3$ Activation by Phosphine Ligands. *Chem. Commun.* **2017**, *53*, 854–856. https://doi.org/10.1039/C6CC08824D.

(27) Thomas, G. T.; Janusson, E.; Zijlstra, H. S.; McIndoe, J. S. Step-by-Step Real Time Monitoring of a Catalytic Amination Reaction. *Chem. Commun.* **2019**, *55*, 11727–11730. https://doi.org/10.1039/C9CC05076K.

(28) Li, H.; Grasa, G. A.; Colacot, T. J. A Highly Efficient, Practical, and General Route for the Synthesis of (R$_3$P)$_2$Pd(0): Structural Evidence on the Reduction Mechanism of Pd(II) to Pd(0). *Org. Lett.* **2010**, *12*, 3332–3335. https://doi.org/10.1021/ol101106z.

(29) MacQueen, P. M.; Holley, R.; Ghorai, S.; Colacot, T. J. Convenient One-Pot Synthesis of L$_2$Pd(0) Complexes for Cross-Coupling Catalysis. *Organometallics* **2023**, *42*, 2644–2650. https://doi.org/10.1021/acs.organomet.3c00059.

(30) Andreu, M. G.; Zapf, A.; Beller, M. Molecularly Defined Palladium(0) Monophosphine Complexes as Catalysts for Efficient Cross-Coupling of Aryl Chlorides and Phenylboronic Acid. *Chem. Commun.* **2000**, 2475–2476. https://doi.org/10.1039/B006791L.

(31) Lee, H. G.; Milner, P. J.; Buchwald, S. L. An Improved Catalyst System for the Pd-Catalyzed Fluorination of (Hetero)Aryl Triflates. *Org. Lett.* **2013**, *15*, 5602–5605. https://doi.org/10.1021/ol402859k.

(32) Lee, H. G.; Milner, P. J.; Buchwald, S. L. Pd-Catalyzed Nucleophilic Fluorination of Aryl Bromides. *J. Am. Chem. Soc.* **2014**, *136*, 3792–3795. https://doi.org/10.1021/ja5009739.

(33) Lee, H. G.; Milner, P. J.; Colvin, M. T.; Andreas, L.; Buchwald, S. L. Structure and Reactivity of [(L·Pd)$_n$·(1,5-Cyclooctadiene)] (n=1–2) Complexes Bearing Biaryl Phosphine Ligands. *Inorg. Chim. Acta* **2014**, *422*, 188–192. https://doi.org/10.1016/j.ica.2014.06.008.

(34) Neff, R. K.; Frantz, D. E. Cationic Alkynyl Heck Reaction toward Substituted Allenes Using BobCat: A New Hybrid Pd(0)-Catalyst Incorporating a Water-Soluble dba Ligand. *J. Am. Chem. Soc.* **2018**, *140*, 17428–17432. https://doi.org/10.1021/jacs.8b11759.

(35) Sato, R.; Kanbara, T.; Kuwabara, J. Synthesis of an Air-Stable Pd(0) Catalyst Bearing Donor and Acceptor Phosphine Ligands. *Organometallics* **2020**, *39*, 235–238. https://doi.org/10.1021/acs.organomet.9b00646.

(36) Sato, R.; Kanbara, T.; Kuwabara, J. Air-Stable Pd(0) Catalyst Bearing Dual Phosphine Ligands: A Detailed Evaluation of Air Stability and Catalytic Property in Cross-Coupling Reactions. *Dalton Trans.* **2020**, *49*, 12814–12819. https://doi.org/10.1039/D0DT02744H.

(37) Huang, J.; Isaac, M.; Watt, R.; Becica, J.; Dennis, E.; Saidaminov, M. I.; Sabbers, W. A.; Leitch, D. C. ^{DMP}DAB–Pd–MAH: A Versatile Pd(0) Source for Precatalyst Formation, Reaction Screening, and Preparative-Scale Synthesis. *ACS Catal.* **2021**, *11*, 5636–5646. https://doi.org/10.1021/acscatal.1c00288.

(38) Pipaón Fernández, N.; Gaube, G.; Woelk, K. J.; Burns, M.; Hruszkewycz, D. P.; Leitch, D. C. Palladium-Catalyzed Direct C–H Alkenylation with Enol Pivalates Proceeds via Reversible C–O Oxidative Addition to Pd(0). *ACS Catal.* **2022**, *12*, 6997–7003. https://doi.org/10.1021/acscatal.2c01305.

(39) Richard, F.; Aubert, S.; Katsina, T.; Reinalda, L.; Palomas, D.; Crespo-Otero, R.; Huang, J.; Leitch, D. C.; Mateos, C.; Arseniyadis, S. Enantioselective Synthesis of γ-Butenolides through Pd-Catalysed C5-Selective Allylation of Siloxyfurans. *Nat. Synth.* **2022**, *1*, 641–648. https://doi.org/10.1038/s44160-022-00109-1.

(40) Huang, J.; Keenan, T.; Richard, F.; Lu, J.; Jenny, S. E.; Jean, A.; Arseniyadis, S.; Leitch, D. C. Chiral, Air Stable, and Reliable Pd(0) Precatalysts Applicable to Asymmetric Allylic Alkylation Chemistry. *Nat. Commun.* **2023**, *14*, 8058. https://doi.org/10.1038/s41467-023-43512-8.

(41) Bigler, R.; Spiess, D.; Wellauer, J.; Binder, M.; Carré, V.; Fantasia, S. Synthesis of Biaryl Phosphine Palladium(0) Precatalysts. *Organometallics* **2021**, *40*, 2384–2388. https://doi.org/10.1021/acs.organomet.1c00288.

(42) Cavell, K. J.; Stufkens, D. J.; Vrieze, K. 1,4-Diazabutadiene Olefin Complexes of Zerovalent Palladium: Preparation and Characterization. *Inorg. Chim. Acta* **1981**, *47*, 67–76. https://doi.org/10.1016/S0020-1693(00)89309-3.

(43) Tempel, D. J.; Johnson, L. K.; Huff, R. L.; White, P. S.; Brookhart, M. Mechanistic Studies of Pd(II)−α-Diimine-Catalyzed Olefin Polymerizations. *J. Am. Chem. Soc.* **2000**, *122*, 6686–6700. https://doi.org/10.1021/ja000893v.

(44) Poli, R.; Nguyen, D.; Liu, Y.-S.; Harth, E. Homolytic Pd^{II}–C Bond Cleavage in the MILRad Process: Reversibility and Termination Mechanism. *Organometallics* **2023**, *42*, 2277–2286. https://doi.org/10.1021/acs.organomet.3c00277.

(45) Eagan, J. M.; Padilla-Vélez, O.; O'Connor, K. S.; MacMillan, S. N.; LaPointe, A. M.; Coates, G. W. Chain-Straightening Polymerization of Olefins to Form Polar Functionalized Semicrystalline Polyethylene. *Organometallics* **2022**, *41*, 3411–3418. https://doi.org/10.1021/acs.organomet.2c00366.

(46) Zhang, Y.; Zhang, Y.; Hu, X.; Wang, C.; Jian, Z. Advances on Controlled Chain Walking and Suppression of Chain Transfer in Catalytic Olefin Polymerization. *ACS Catal.* **2022**, *12*, 14304–14320. https://doi.org/10.1021/acscatal.2c04272.

(47) Lu, W.; Wang, H.; Fan, W.; Dai, S. Exploring the Relationship between the Polyethylene Microstructure and Spatial Structure of α-Diimine Pd(II) Catalysts via a Hybrid Steric Strategy. *Inorg. Chem.* **2022**, *61*, 6799–6806. https://doi.org/10.1021/acs.inorgchem.1c03969.

(48) Gies, A. P.; Zhou, Z.; Mukhopadhyay, S.; Kosanovich, A. J.; Keaton, R. J.; Auyeung, E.; Kobylianskii, I.; Beezer, D. B.; Dau, H.; Harth, E. Analytical Insights into the Microstructures and Reaction Mechanisms of Cationic Pd(II) α-Diimine-Catalyzed Polyolefins. *Macromolecules* **2021**, *54*, 10814–10829. https://doi.org/10.1021/acs.macromol.1c01478.

(49) Wang, X.; Dong, B.; Yang, Q.; Liu, H.; Hu, Y.; Zhang, X. Boosting the Thermal Stability of α-Diimine Palladium Complexes in Norbornene Polymerization from Construction of Intraligand Hydrogen Bonding and Simultaneous Increasing Axial/Equatorial Bulkiness. *Inorg. Chem.* **2021**, *60*, 2347–2361. https://doi.org/10.1021/acs.inorgchem.0c03185.

(50) Tran, Q. H.; Wang, X.; Brookhart, M.; Daugulis, O. Cationic α-Diimine Nickel and Palladium Complexes Incorporating Phenanthrene Substituents: Highly Active Ethylene Polymerization Catalysts and Mechanistic Studies of Syn/Anti Isomerization. *Organometallics* **2020**, *39*, 4704–4716. https://doi.org/10.1021/acs.organomet.0c00696.

(51) Takeuchi, D.; Yamada, T.; Nakamaru, Y.; Osakada, K.; Aratani, I.; Suzuki, Y. Pd-Promoted Copolymerization of Methallyl and Isoprenyl Ethers and Acetate with α-Olefins. *Organometallics* **2019**, *38*, 2323–2329. https://doi.org/10.1021/acs.organomet.9b00150.

(52) Liao, Y.; Zhang, Y.; Cui, L.; Mu, H.; Jian, Z. Pentiptycenyl Substituents in Insertion Polymerization with α-Diimine Nickel and Palladium Species. *Organometallics* **2019**, *38*, 2075–2083. https://doi.org/10.1021/acs.organomet.9b00106.

(53) Zhang, Y.; Xia, J.; Song, J.; Zhang, J.; Ni, X.; Jian, Z. Combination of Ethylene, 1,3-Butadiene, and Carbon Dioxide into Ester-Functionalized Polyethylenes via Palladium-Catalyzed Coupling and Insertion Polymerization. *Macromolecules* **2019**, *52*, 2504–2512. https://doi.org/10.1021/acs.macromol.9b00195.

(54) Chen, Z.; Brookhart, M. Exploring Ethylene/Polar Vinyl Monomer Copolymerizations Using Ni and Pd α-Diimine Catalysts. *Acc. Chem. Res.* **2018**, *51*, 1831–1839. https://doi.org/10.1021/acs.accounts.8b00225.

(55) Xu, H.; Hu, C. T.; Wang, X.; Diao, T. Structural Characterization of β-Agostic Bonds in Pd-Catalyzed Polymerization. *Organometallics* **2017**, *36*, 4099–4102. https://doi.org/10.1021/acs.organomet.7b00666.

(56) Zhao, M.; Chen, C. Accessing Multiple Catalytically Active States in Redox-Controlled Olefin Polymerization. *ACS Catal.* **2017**, *7*, 7490–7494. https://doi.org/10.1021/acscatal.7b02564.

(57) Zhai, F.; Solomon, J. B.; Jordan, R. F. Copolymerization of Ethylene with Acrylate Monomers by Amide-Functionalized α-Diimine Pd Catalysts. *Organometallics* **2017**, *36*, 1873–1879. https://doi.org/10.1021/acs.organomet.7b00209.

12

(58) Kocen, A. L.; Klimovica, K.; Brookhart, M.; Daugulis, O. Alkene Isomerization by "Sandwich" Diimine-Palladium Catalysts. *Organometallics* **2017**, *36*, 787–790. https://doi.org/10.1021/acs.organomet.6b00856.

(59) Crociani, B.; Bianca, F. D.; Uguagliati, P.; Canovese, L.; Berton, A. Phenylation of Cationic Allyl Palladium(II) Complexes by Tetraphenylborate. Synthesis of α-Diimine Olefin Palladium(0) Complexes and Mechanistic Aspects. *J. Chem. Soc. Dalton Trans.* **1991**, 71–79. https://doi.org/10.1039/DT9910000071.

(60) Raoufmoghaddam, S.; Mannathan, S.; Minnaard, A. J.; de Vries, J. G.; de Bruin, B.; Reek, J. N. H. Importance of the Reducing Agent in Direct Reductive Heck Reactions. *ChemCatChem* **2018**, *10*, 266–272. https://doi.org/10.1002/cctc.201701206.

(61) Lee, J.-Y.; Shen, J.-S.; Tzeng, R.-J.; Lu, I.-C.; Lii, J.-H.; Hu, C.-H.; Lee, H. M. Well-Defined Palladium(0) Complexes Bearing N-Heterocyclic Carbene and Phosphine Moieties: Efficient Catalytic Applications in the Mizoroki–Heck Reaction and Direct C–H Functionalization. *Dalton Trans.* **2016**, *45*, 10375–10388. https://doi.org/10.1039/C6DT01323F.

(62) Raoufmoghaddam, S.; Mannathan, S.; Minnaard, A. J.; de Vries, J. G.; Reek, J. N. H. Palladium(0)/NHC-Catalyzed Reductive Heck Reaction of Enones: A Detailed Mechanistic Study. *Chem. Eur. J.* **2015**, *21*, 18811–18820. https://doi.org/10.1002/chem.201503217.

(63) Jhou, Y.-M.; Nandi, D.; Lee, J.-Y.; Tzeng, R.-J.; Lee, H. M. Palladium(0) Complexes of N-Heterocyclic Carbene Ligands with Dangling NMeCO Functionalities: Synthesis, Reactivity and Application in Mizoroki–Heck Reactions. *Polyhedron* **2015**, *100*, 28–35. https://doi.org/10.1016/j.poly.2015.07.027.

(64) Lee, J.-Y.; Cheng, P.-Y.; Tsai, Y.-H.; Lin, G.-R.; Liu, S.-P.; Sie, M.-H.; Lee, H. M. Efficient Heck Reactions Catalyzed by Palladium(0) and -(II) Complexes Bearing N-Heterocyclic Carbene and Amide Functionalities. *Organometallics* **2010**, *29*, 3901–3911. https://doi.org/10.1021/om1006402.

(65) Warsink, S.; Bosman, S.; Weigand, J. J.; Elsevier, C. J. Rigid Pyridyl Substituted NHC Ligands, Their Pd(0) Complexes and Their Application in Selective Transfer Semihydrogenation of Alkynes. *Appl. Organomet. Chem.* **2011**, *25*, 276–282. https://doi.org/10.1002/aoc.1754.

(66) Warsink, S.; Chang, I.-H.; Weigand, J. J.; Hauwert, P.; Chen, J.-T.; Elsevier, C. J. NHC Ligands with a Secondary Pyrimidyl Donor for Electron-Rich Palladium(0) Complexes. *Organometallics* **2010**, *29* (20), 4555–4561. https://doi.org/10.1021/om100670u.

(67) Warsink, S.; Hauwert, P.; Siegler, M. A.; Spek, A. L.; Elsevier, C. J. Palladium(0) Pre-Catalysts with Heteroditopic NHC–Amine Ligands by Transmetallation from Their Silver(I) Complexes. *Appl. Organomet. Chem.* **2009**, *23*, 225–228. https://doi.org/10.1002/aoc.1501.

(68) Hauwert, P.; Boerleider, R.; Warsink, S.; Weigand, J. J.; Elsevier, C. J. Mechanism of Pd(NHC)-Catalyzed Transfer Hydrogenation of Alkynes. *J. Am. Chem. Soc.* **2010**, *132* (47), 16900–16910. https://doi.org/10.1021/ja1062407.

(69) Sluijter, S. N.; Warsink, S.; Lutz, M.; Elsevier, C. J. Synthesis of Palladium(0) and -(II) Complexes with Chelating Bis(N-Heterocyclic Carbene) Ligands and Their Application in Semihydrogenation. *Dalton Trans.* **2013**, *42*, 7365–7372. https://doi.org/10.1039/C3DT32835J.

(70) de Pater, J. J. M.; Tromp, D. S.; Tooke, D. M.; Spek, A. L.; Deelman, B.-J.; van Koten, G.; Elsevier, C. J. Palladium(0)-Alkene Bis(Triarylphosphine) Complexes as Catalyst Precursors for the Methoxycarbonylation of Styrene. *Organometallics* **2005**, *24*, 6411–6419. https://doi.org/10.1021/om0506419.

(71) de Pater, Jeroen. J. M.; Maljaars, C. E. P.; de Wolf, E.; Lutz, M.; Spek, A. L.; Deelman, B.-J.; Elsevier, C. J.; van Koten, G. (Perfluoro)Alkylsilyl-Substituted 2-[Bis(4-Aryl)Phosphino]Pyridines: Synthesis and Comparison of Their Palladium Complexes in Methoxycarbonylation of Phenylacetylene in Regular Solvents and Supercritical CO₂. *Organometallics* **2005**, *24*, 5299–5310. https://doi.org/10.1021/om050479+.

(72) Ferrara, M. L.; Giordano, F.; Orabona, I.; Panunzi, A.; Ruffo, F. [Pd(N,N-Chelate)(Olefin)] Complexes Containing Chiral Nitrogen Chelates Based on Carbohydrates – Enantioselectivity of Olefin Coordination. *Eur. J. Inorg. Chem.* **1999**, 1939–1947. https://doi.org/10.1002/(SICI)1099-0682(199911)1999:11<1939::AID-EJIC1939>3.0.CO;2-2.

(73) Yoshida, T.; Otsuka, S. Reactions of Two-Coordinate Phosphine Platinum(0) and Palladium(0) Compounds. Ligand Exchange and Reactivities toward Small Molecules. *J. Am. Chem. Soc.* **1977**, *99*, 2134–2140. https://doi.org/10.1021/ja00449a019.

(74) Ozawa, F.; Ito, T.; Nakamura, Y.; Yamamoto, A. Palladium(0) Complexes Coordinated with Substituted Olefins and Tertiary Phosphine Ligands. *J. Organomet. Chem.* **1979**, *168*, 375–391. https://doi.org/10.1016/S0022-328X(00)83219-2.

(75) Canovese, L.; Visentin, F.; Levi, C.; Dolmella, A. Synthesis, Characterization, Dynamics and Reactivity toward Amination of η³-Allyl Palladium Complexes Bearing Mixed Ancillary Ligands. Evaluation of the Electronic Characteristics of the Ligands from Kinetic Data. *Dalton Trans.* **2011**, *40*, 966–981. https://doi.org/10.1039/C0DT00811G.

(76) Komine, N.; Ito, R.; Suda, H.; Hirano, M.; Komiya, S. Selective Alkene Insertion into Inert Hydrogen–Metal Bonds Catalyzed by Mono(Phosphorus Ligand)Palladium(0) Complexes. *Organometallics* **2017**, *36*, 4160–4168. https://doi.org/10.1021/acs.organomet.7b00593.

(77) Scattolin, T.; Pangerc, N.; Lampronti, I.; Tupini, C.; Gambari, R.; Marvelli, L.; Rizzolio, F.; Demitri, N.; Canovese, L.; Visentin, F. Palladium (0) Olefin Complexes Bearing Purine-Based N-Heterocyclic Carbenes and 1,3,5-Triaza-7-Phosphaadamantane (PTA): Synthesis, Characterization and Antiproliferative Activity toward Human Ovarian Cancer Cell Lines. *J. Organomet. Chem.* **2019**, *899*, 120857. https://doi.org/10.1016/j.jorganchem.2019.07.008.

(78) Diversi, P.; Ingrosso, G.; Lucherini, A. Metallacycloalkane Chemistry: Synthesis of the First Palladacyclopentane Derivative and its Transformation into a η³-Butenyl Cationic Complex. *J. Chem. Soc. Chem. Commun.* **1978**, 735–736. https://doi.org/10.1039/C39780000735.

(79) Jedlicka, B.; Rülke, R. E.; Weissensteiner, W.; Fernández-Galán, R.; Jalón, F. A.; Manzano, B. R.; Rodríguez-de la Fuente, J.; Veldman, N.; Kooijman, H.; Spek, A. L. Synthesis and Molecular Structures of Palladium and Platinum Complexes of PTFA: Models of Grignard Cross-Coupling Catalysts. *J. Organomet. Chem.* **1996**, *516*, 97–110. https://doi.org/10.1016/0022-328X(95)06044-W.

(80) Fernández-Galán, R.; Jalón, F. A.; Manzano, B. R.; Rodríguez-de la Fuente, J.; Vrahami, M.; Jedlicka, B.; Weissensteiner, W.; Jogl, G. New Chiral Palladium(0) and -(II) Complexes of (Aminoferrocenyl)Phosphine Ligands PPFA and PTFA. X-Ray Crystal Structure Analysis and Fluxional Behavior Involving Alkene Rotation, Pd−N Bond Rupture, and Selective η3−η1−η3 Allyl Isomerization. *Organometallics* **1997**, *16*, 3758–3768. https://doi.org/10.1021/om9610354.

(81) Antonaroli, S.; Crociani, B. Preparation and Reactions of Palladium(0)–Olefin Complexes with Iminophosphine Ligands. *J. Organomet. Chem.* **1998**, *560*, 137–146. https://doi.org/10.1016/S0022-328X(98)00472-0.

(82) van Laren, M. W.; Elsevier, C. J. Selective Homogeneous Palladium(0)-Catalyzed Hydrogenation of Alkynes to (Z)-Alkenes. *Angew. Chem. Int. Ed.* **1999**, *38*, 3715–3717. https://doi.org/10.1002/(SICI)1521-3773(19991216)38:24<3715::AID-ANIE3715>3.0.CO;2-O.

(83) Manzano, B. R.; Jalón, F. A.; Gómez-de la Torre, F.; López-Agenjo, A. M.; Rodríguez, A. M.; Mereiter, K.; Weissensteiner, W.; Sturm, T. Novel BPPFA Palladium Complexes. P,P to P,N Rearrangements Promoted by Chelating κ³-N,P,P-BPPFA Intermediates. *Organometallics* **2002**, *21*, 789–802. https://doi.org/10.1021/om010656g.

(84) Crociani, B.; Antonaroli, S.; Beghetto, V.; Matteoli, U.; Scrivanti, A. Mechanistic Study on the Cross-Coupling of Alkynyl Stannanes with Aryl Iodides Catalyzed by η²-(Dimethyl Fumarate)Palladium(0) Complexes with Iminophosphine Ligands. *Dalton Trans.* **2003**, 2194–2202. https://doi.org/10.1039/B300020F.

(85) Carrión, M. C.; Jalón, F. A.; López-Agenjo, A.; Manzano, B. R.; Weissensteiner, W.; Mereiter, K. Pd(0) and Pd(II) Derivatives with Heteroannularly Bridged Chiral Ferrocenyl Diphosphine Ligands

13

– A Stereochemical Analysis. *J. Organomet. Chem.* **2006**, *691*, 1369–1381. https://doi.org/10.1016/j.jorganchem.2005.12.023.

(86)   Canovese, L.; Visentin, F.; Chessa, G.; Uguagliati, P.; Santo, C.; Maini, L. The Synthesis of Palladacyclopentadienyl Derivatives from Rigid Bis-Alkynes and Their Use as Precursors in the Synthesis of Fluoroanthene-like Cycles under Mild Conditions. A Reactivity Investigation. *J. Organomet. Chem.* **2007**, *692*, 2342–2345. https://doi.org/10.1016/j.jorganchem.2007.01.046.

(87)   Canovese, L.; Santo, C.; Visentin, F. Palladium(0)-Catalyzed Cis−Trans Alkene Isomerizations. *Organometallics* **2008**, *27*, 3577–3581. https://doi.org/10.1021/om800305h.

(88)   Plessow, P. N.; Weigel, L.; Lindner, R.; Schäfer, A.; Rominger, F.; Limbach, M.; Hofmann, P. Mechanistic Details of the Nickel-Mediated Formation of Acrylates from CO_2, Ethylene and Methyl Iodide. *Organometallics* **2013**, *32*, 3327–3338. https://doi.org/10.1021/om400262b.

(89)   Canovese, L.; Scattolin, T.; Visentin, F.; Santo, C. Reactions of Palladium(0) Olefin Complexes Stabilized by Some Different Hetero- and Homo-Ditopic Spectator Ligands with Propargyl Halides. *J. Organomet. Chem.* **2017**, *834*, 10–21. https://doi.org/10.1016/j.jorganchem.2017.02.003.

(90)   Echavarren, A. M.; Stille, J. K. On the Preparation of Tris(Tribenzyldeneacetylacetone)Tripalladium: A Correction. *J. Organomet. Chem.* **1988**, *356*, C35–C37. https://doi.org/10.1016/0022-328X(88)80689-2.

(91)   Marsh, R. E.; Ubell, E.; Wilcox, H. E. The Crystal Structure of Maleic Anhydride. *Acta Crystallogr.* **1962**, *15*, 35–41. https://doi.org/10.1107/S0365110X62000080.

(92)   Silva, B. P.; Costa, A. G. L.; da Silva, M. B.; Cunha, A. M.; Santos, R. C. R.; Valentini, A.; Zanatta, G.; de Lima-Neto, P.; Caetano, E. W. S.; Freire, V. N. Dimethyl Fumarate Molecule, Crystal, and Plane: Optical Absorption Measurement and Structural/Optoelectronic Properties by Density Functional Theory Calculations. *J. Phys. Chem. Solids* **2022**, *170*, 110958. https://doi.org/10.1016/j.jpcs.2022.110958.

(93)   Ingoglia, B. T.; Buchwald, S. L. Oxidative Addition Complexes as Precatalysts for Cross-Coupling Reactions Requiring Extremely Bulky Biarylphosphine Ligands. *Org. Lett.* **2017**, *19*, 2853–2856. https://doi.org/10.1021/acs.orglett.7b01082.

(94)   Uehling, M. R.; King, R. P.; Krska, S. W.; Cernak, T.; Buchwald, S. L. Pharmaceutical Diversification via Palladium Oxidative Addition Complexes. *Science* **2019**, *363*, 405–408. https://doi.org/10.1126/science.aac6153.

(95)   Mallek, A. J.; Pentelute, B. L.; Buchwald, S. L. Selective N-Arylation of p-Aminophenylalanine in Unprotected Peptides with Organometallic Palladium Reagents. *Angew. Chem. Int. Ed.* **2021**, *60*, 16928–16931. https://doi.org/10.1002/anie.202104780.

(96)   Timsina, Y. N.; Xu, G.; Colacot, T. J. It Is Not All about the Ligands: Exploring the Hidden Potentials of tBu₃P through Its Oxidative Addition Complex as the Precatalyst. *ACS Catal.* **2023**, *13*, 8106–8118. https://doi.org/10.1021/acscatal.3c01582.

(97)   Mitchell, E. A.; Jessop, P. G.; Baird, M. C. A Kinetics Study of the Oxidative Addition of Bromobenzene to Pd(PCy₃)₂ (Cy = Cyclohexyl) in a Nonpolar Medium: The Influence on Rates of Added PCy₃ and Bromide Ion. *Organometallics* **2009**, *28*, 6732–6738. https://doi.org/10.1021/om900679w.

(98)   Barrios-Landeros, F.; Hartwig, J. F. Distinct Mechanisms for the Oxidative Addition of Chloro-, Bromo-, and Iodoarenes to a Bisphosphine Palladium(0) Complex with Hindered Ligands. *J. Am. Chem. Soc.* **2005**, *127*, 6944–6945. https://doi.org/10.1021/ja042959i.

(99)   Barrios-Landeros, F.; Carrow, B. P.; Hartwig, J. F. Effect of Ligand Steric Properties and Halide Identity on the Mechanism for Oxidative Addition of Haloarenes to Trialkylphosphine Pd(0) Complexes. *J. Am. Chem. Soc.* **2009**, *131*, 8141–8154. https://doi.org/10.1021/ja900798s.

(100)   Lu, J.; Donnecke, S.; Paci, I.; Leitch, D. C. A Reactivity Model for Oxidative Addition to Palladium Enables Quantitative Predictions for Catalytic Cross-Coupling Reactions. *Chem. Sci.* **2022**, *13*, 3477–3488. https://doi.org/10.1039/D2SC00174H.

(101)   Amatore, C.; Jutand, A.; Khalil, F.; M'Barki, M. A.; Mottier, L. Rates and Mechanisms of Oxidative Addition to Zerovalent Palladium Complexes Generated in Situ from Mixtures of Pd⁰(dba)₂ and Triphenylphosphine. *Organometallics* **1993**, *12*, 3168–3178. https://doi.org/10.1021/om00032a045.

(102)   Macé, Y.; Kapdi, A. R.; Fairlamb, I. J. S.; Jutand, A. Influence of the dba Substitution on the Reactivity of Palladium(0) Complexes Generated from Pd⁰₂(dba-*n*,*n*'-Z)₃ or Pd⁰(dba-*n*,*n*'-Z)₂ and PPh₃ in Oxidative Addition with Iodobenzene. *Organometallics* **2006**, *25*, 1795–1800. https://doi.org/10.1021/om0510876.

(103)   King, R. P.; Krska, S. W.; Buchwald, S. L. A Neophyl Palladacycle as an Air- and Thermally Stable Precursor to Oxidative Addition Complexes. *Org. Lett.* **2021**, *23*, 7927–7932. https://doi.org/10.1021/acs.orglett.1c02307.

(104)   Littke, A. F.; Fu, G. C. A Versatile Catalyst for Heck Reactions of Aryl Chlorides and Aryl Bromides under Mild Conditions. *J. Am. Chem. Soc.* **2001**, *123*, 6989–7000. https://doi.org/10.1021/ja010988c.

(105)   J. Scott, N. W.; J. Ford, M.; Schotes, C.; R. Parker, R.; C. Whitwood, A.; S. Fairlamb, I. J. The Ubiquitous Cross-Coupling Catalyst System 'Pd(OAc)₂'/2PPh₃ Forms a Unique Dinuclear Pdᴵ Complex: An Important Entry Point into Catalytically Competent Cyclic Pd₃ Clusters. *Chem. Sci.* **2019**, *10*, 7898–7906. https://doi.org/10.1039/C9SC01847F.

(106)   Neeve, E. C.; Geier, S. J.; Mkhalid, I. A. I.; Westcott, S. A.; Marder, T. B. Diboron(4) Compounds: From Structural Curiosity to Synthetic Workhorse. *Chem. Rev.* **2016**, *116*, 9091–9161. https://doi.org/10.1021/acs.chemrev.6b00193.

(107)   Arrington, K.; Barcan, G. A.; Calandra, N. A.; Erickson, G. A.; Li, L.; Liu, L.; Nilson, M. G.; Strambeanu, I. I.; VanGelder, K. F.; Woodard, J. L.; Xie, S.; Allen, C. L.; Kowalski, J. A.; Leitch, D. C. Convergent Synthesis of the NS5B Inhibitor GSK8175 Enabled by Transition Metal Catalysis. *J. Org. Chem.* **2019**, *84*, 4680–4694. https://doi.org/10.1021/acs.joc.8b02269.

(108)   Munteanu, C.; Spiller, T. E.; Qiu, J.; DelMonte, A. J.; Wisniewski, S. R.; Simmons, E. M.; Frantz, D. E. Pd- and Ni-Based Systems for the Catalytic Borylation of Aryl (Pseudo)Halides with B₂(OH)₄. *J. Org. Chem.* **2020**, *85*, 10334–10349. https://doi.org/10.1021/acs.joc.0c00929.

(109)   Ring, O. T.; Campbell, A. D.; Hayter, B. R.; Powell, L. Significant Rate Enhancement via Potassium Pivalate in a Miyaura Borylation Approach to Verinurad. *Tet. Lett.* **2020**, *61*, 151589. https://doi.org/10.1016/j.tetlet.2019.151589.

(110)   Gaube, G.; Fernandez, N. P.; Leitch, D. C. An Evaluation of Palladium-Based Catalysts for the Base-Free Borylation of Alkenyl Carboxylates. *New J. Chem.* **2021**, *45*, 20095–20098. https://doi.org/10.1039/D1NJ04008A.

(111)   Wei, C. S.; Davies, G. H. M.; Soltani, O.; Albrecht, J.; Gao, Q.; Pathirana, C.; Hsiao, Y.; Tummala, S.; Eastgate, M. D. The Impact of Palladium(II) Reduction Pathways on the Structure and Activity of Palladium(0) Catalysts. *Angew. Chem. Int. Ed.* **2013**, *52*, 5822–5826. https://doi.org/10.1002/anie.201210252.

(112)   Dymicky, M.; Buchanan, R. L. Preparation of n-Monoalkyl Maleates and n-Mono- and Dialkyl Fumarates. *Org. Prep. Proced. Int.* **1985**, *17*, 121–131. https://doi.org/10.1080/00304948509355484.

(113)   Shimomaki, K.; Murata, K.; Martin, R.; Iwasawa, N. Visible-Light-Driven Carboxylation of Aryl Halides by the Combined Use of Palladium and Photoredox Catalysts. *J. Am. Chem. Soc.* **2017**, *139*, 9467–9470. https://doi.org/10.1021/jacs.7b04838.

(114)   Abrams, M. B.; Scott, B. L.; Baker, R. T. Sterically Tunable Phosphenium Cations: Synthesis and Characterization of Bis(Arylamino)Phosphenium Ions, Phosphinophosphenium Adducts, and the First Well-Defined Rhodium Phosphenium Complexes. *Organometallics* **2000**, *19*, 4944–4956. https://doi.org/10.1021/om0005351.

(115)   Zheng, J.; Yao, Y.; Li, M.; Wang, L.; Zhang, X. A Non-MPD-Type Reverse Osmosis Membrane with Enhanced Permselectivity for Brackish Water Desalination. *J. Membr. Sci.* **2018**, *565*, 104–111. https://doi.org/10.1016/j.memsci.2018.08.015.

(116)   Huang, J.; Ho, B. D.; Gaube, G.; Celuszak, H.; Becica, J.; Schley, N. D.; Leitch, D. C. A Thermally Stable, Alkene-Free Palladium Source for Oxidative Addition Complex Formation and High Turnover Catalysis. *ChemRxiv* **2024**, https://doi.org/10.26434/chemrxiv-2024-ml7